

# Assessment of fat-specific protein 27 in the adipocyte lineage suggests a dual role for FSP27 in adipocyte metabolism and cell death

Ji Young Kim, Kun Liu, Shengli Zhou, Kristin Tillison, Yu Wu and Cynthia M. Smas

*Am J Physiol Endocrinol Metab* 294:E654-E667, 2008. First published 15 January 2008;  
doi:10.1152/ajpendo.00104.2007

**You might find this additional info useful...**

Supplemental material for this article can be found at:

<http://ajpendo.physiology.org/content/suppl/2008/02/13/00104.2007.DC1.html>

This article cites 58 articles, 33 of which can be accessed free at:

<http://ajpendo.physiology.org/content/294/4/E654.full.html#ref-list-1>

This article has been cited by 5 other HighWire hosted articles

**Differential regulation of CIDEA and CIDEA expression by insulin via Akt1/2- and JNK2-dependent pathways in human adipocytes**

Minoru Ito, Michiaki Nagasawa, Naoki Omae, Tomohiro Ide, Yunike Akasaka and Koji Murakami

*J. Lipid Res.*, August, 2011; 52 (8): 1450-1460.

[\[Abstract\]](#) [\[Full Text\]](#) [\[PDF\]](#)

**Regulation of fat specific protein 27 by isoproterenol and TNF- $\alpha$  to control lipolysis in murine adipocytes**

Srijana Ranjit, Emilie Boutet, Pallavi Gandhi, Matthieu Prot, Yoshikazu Tamori, Anil Chawla, Andrew S. Greenberg, Vishwajeet Puri and Michael P. Czech

*J. Lipid Res.*, February, 2011; 52 (2): 221-236.

[\[Abstract\]](#) [\[Full Text\]](#) [\[PDF\]](#)

**Differential roles of CIDEA and CIDEA in insulin-induced anti-apoptosis and lipid droplet formation in human adipocytes**

Minoru Ito, Michiaki Nagasawa, Tomoko Hara, Tomohiro Ide and Koji Murakami

*J. Lipid Res.*, July, 2010; 51 (7): 1676-1684.

[\[Abstract\]](#) [\[Full Text\]](#) [\[PDF\]](#)

**Functional analysis of FSP27 protein regions for lipid droplet localization, caspase-dependent apoptosis, and dimerization with CIDEA**

Kun Liu, Shengli Zhou, Ji-Young Kim, Kristin Tillison, David Majors, David Rearick, Jun Ho Lee, Ruby F. Fernandez-Boyanapalli, Katherine Barricklow, M. Sue Houston and Cynthia M. Smas

*Am J Physiol Endocrinol Metab*, December, 2009; 297 (6): E1395-E1413.

[\[Abstract\]](#) [\[Full Text\]](#) [\[PDF\]](#)

**A Functional Interaction between RIP140 and PGC-1 $\alpha$  Regulates the Expression of the Lipid Droplet Protein CIDEA**

Magnus Hallberg, Daniel L. Morganstein, Evangelos Kiskinis, Kunal Shah, Anastasia Kralli, Stephen M. Dilworth, Roger White, Malcolm G. Parker and Mark Christian

*Mol. Cell. Biol.* 2008; 28 (22): 6785-6795.

[\[Abstract\]](#) [\[Full Text\]](#) [\[PDF\]](#)

Updated information and services including high resolution figures, can be found at:

<http://ajpendo.physiology.org/content/294/4/E654.full.html>

Additional material and information about *AJP - Endocrinology and Metabolism* can be found at:

<http://www.the-aps.org/publications/ajpendo>

---

This information is current as of October 21, 2011.

## Assessment of fat-specific protein 27 in the adipocyte lineage suggests a dual role for FSP27 in adipocyte metabolism and cell death

Ji Young Kim,\* Kun Liu,\* Shengli Zhou, Kristin Tillison, Yu Wu, and Cynthia M. Smas

Department of Biochemistry and Cancer Biology, University of Toledo Health Science Campus, Toledo, Ohio

Submitted 15 February 2007; accepted in final form 6 January 2008

**Kim JY, Liu K, Zhou S, Tillison K, Wu Y, Smas CM.** Assessment of fat-specific protein 27 in the adipocyte lineage suggests a dual role for FSP27 in adipocyte metabolism and cell death. *Am J Physiol Endocrinol Metab* 294: E654–E667, 2008. First published January 15, 2008; doi:10.1152/ajpendo.00104.2007.—Fat-specific protein 27 (FSP27)/CIDE was initially identified by its upregulation in TA1 adipogenesis and is one of three cell death-inducing DFF45-like effector (CIDE) family proapoptotic proteins. Ectopic expression of CIDEs promotes apoptosis of mammalian cells. On the other hand, FSP27 has very recently been illustrated to regulate lipid droplet size and promote lipid storage in adipocytes. Regulation of endogenous FSP27 expression is unknown. We assessed the FSP27 transcript level in the well-characterized 3T3-L1 in vitro adipocyte differentiation model and found its emergence parallels the adipocyte-enriched transcript adipocyte fatty acid binding protein and stearoyl Co-A desaturase 1. Furthermore, FSP27 is a differentiation-dependent transcript in adipogenesis of primary rodent and human preadipocytes and in brown adipogenesis. The FSP27 transcript is inversely regulated by TNF- $\alpha$  and insulin, consistent with an antilipolytic function. It is nearly abolished with a 4-h exposure of 3T3-L1 adipocytes to 10 ng/ml TNF- $\alpha$ , while treatment with 100 nM insulin increased the FSP27 transcript eightfold. In the latter case LY-294002 blocked this response, indicating involvement of phosphatidylinositol 3-kinase signals. Northern blot analysis of murine tissues indicated exclusive expression of FSP27 in white and brown adipose tissue; however, a dramatic upregulation occurred in the liver of *ob/ob* mice. Ectopic expression of murine FSP27 in 293T cells and in 3T3-L1 preadipocytes led to the appearance of key apoptotic hallmarks and cell death. However, despite the upregulation for FSP27 in adipogenesis, we failed to detect DNA laddering indicative of apoptosis in 3T3-L1 adipocytes. This suggests that adipogenesis is accompanied by decreased susceptibility to the proapoptotic effects of FSP27. Overall, our findings support roles for FSP27 in cell death and in adipocyte function.

insulin; tumor necrosis factor- $\alpha$ ; adipogenesis; cell death-inducing DFF45-like effector; apoptosis; 3T3-L1

THE PRIMARY METABOLIC ROLE of white adipocytes is the storage of excess energy as triglyceride and its mobilization to meet energy needs. White adipose tissue (WAT) is also an endocrine organ that synthesizes and secretes of a number of soluble factors, some of which are adipocyte derived such as leptin, resistin, and TNF- $\alpha$  (4, 9, 19, 23). Mature adipocytes arise via differentiation of adipocyte precursors present in adipose tissue (3, 12, 16, 17, 32). For the past several decades, in vitro preadipocyte cell lines, primarily 3T3-L1, have been extensively used to define genes central to the adipocyte phenotype and adipogenesis (15, 17). Adipogenesis is accompanied by

upregulation for genes encoding proteins critical for lipogenesis, lipolysis, lipid transport, insulin sensitivity, hormone signaling, and other adipocyte functions (41). A variety of in vitro and in vivo studies have determined that peroxisome proliferator-activated receptor- $\gamma$  (PPAR $\gamma$ ), a member of the ligand-activated steroid hormone receptor family, is a master transcriptional regulator of the adipogenic program (14, 33, 43–46, 60, 61). The important contribution of the CCAAT-enhancer-binding protein (CEBP) family of transcriptional regulators to adipogenesis has also been firmly established (2, 42, 55, 60, 61).

Fat-specific protein 27 (FSP27) was cloned by Chapman et al. (6) in 1984 via a differential screening approach to identify cDNAs with differentiation-dependent upregulation during in vitro adipogenesis of murine TA1 preadipocytes, and in 1992 they demonstrated that the FSP27 promoter binds CEBP $\alpha$ , confers adipocyte differentiation-dependent expression on a heterologous chloramphenicol acetyl transferase (CAT) reporter gene, and was repressed by TNF- $\alpha$  (11, 59). Until recently, FSP27 was regarded solely as an adipocyte marker gene of unknown function. However, during revision of this article, a study (39) of FSP27 localization and function in 3T3-L1 adipocytes reported that FSP27 is a lipid droplet associated protein that promotes triglyceride deposition in adipocytes by inhibiting lipolysis; as such it appears to be a major new modulator of lipid droplet function that is required for optimal triglyceride storage in adipocytes (39). Knockdown of FSP27 in 3T3-L1 adipocytes was reported to result in the fragmentation of large lipid droplets to produce many small lipid droplets and ectopic expression of FSP27 promoted lipid droplet formation when assessed in 3T3-L1 preadipocytes, COS cells and CHO cells (39). A comprehensive assessment of the expression and the regulation of FSP27 in adipogenesis remains to be investigated. While not yet extensively examined, the human transcript appears to have a somewhat wider expression pattern (29).

The protein sequence and domain structure of FSP27 place it in the cell death-inducing DFF45-like effector (CIDE) protein family (20); this family is comprised of CIDEA, CIDEB, and FSP27 (also known as CIDEA and CIDE3). While ectopic expression studies (19) have demonstrated that CIDE protein expression is sufficient to induce apoptotic cell death, whether CIDEs are indeed an integral or necessary part of the apoptotic death machinery remains to be determined. CIDEs share protein sequence similarities with DNA fragmentation factor 45 (DFF45) in their NH<sub>2</sub>-terminal CIDE N domain (19). Each of the three CIDE proteins also evidence a region of COOH-

\* These authors contributed equally as first authors.

Address for reprint requests and other correspondence: C. M. Smas, Dept. of Biochemistry and Cancer Biology, Univ. of Toledo Health Science Campus, Toledo, OH 43614 (e-mail: cynthia.smas@utoledo.edu).

The costs of publication of this article were defrayed in part by the payment of page charges. The article must therefore be hereby marked “advertisement” in accordance with 18 U.S.C. Section 1734 solely to indicate this fact.

terminal shared homology, the CIDE C domain. Data support a current model whereby CIDE proteins exert a proapoptotic effect via modulation of the actions of the DFF40/DFF45 DNA fragmentation factor complex via CIDE protein sequestration of the inhibitory subunit DFF45 (21, 31), and this leads to the activation of DFF40 nuclease, the major nuclease responsible for the DNA fragmentation that is a classic hallmark of apoptotic cell death (20, 30). The full range and mechanisms of CIDE protein action in apoptosis remain less than fully addressed; however, it appears that in the case of CIDEB, it is the CIDE C domain that is necessary and sufficient for mitochondrial localization and apoptosis (8), when assessed by ectopic expression studies. To date, data on FSP27 function in apoptosis are limited to the observation that ectopic expression of human FSP27 in 293T cells and CHO cells promotes cell death as evidenced by cell morphology and DNA fragmentation (29). The mechanisms underlying this apoptotic response to FSP27 expression are not known. Ectopic expression studies of an EGFP-hFSP27 expression construct in COS cells has revealed that the protein, as has been described for CIDEA and CIDEB, localizes to mitochondria (29). In contrast, a recent study (39) failed to find mitochondrial localization but demonstrated presence of FSP27 protein at adipocyte lipid droplets. This observation is consistent with the previous findings of lipid droplet association for FSP27 during an analysis of the adipocyte lipid droplet proteome (5), although in the latter case this was initially attributed to possible mitochondrial contamination of lipid droplet preparations.

In addition to the recently reported role of FSP27 in lipid droplet function, CIDEA and CIDEB have been firmly established to have a metabolic role in healthy cells. Studies in null mice indicates that CIDEA has a central function in the normal physiology of brown adipose tissue (BAT), where it is key to regulating thermogenesis and energy expenditure via its effect on the activity of the mitochondrial uncoupling protein 1 (UCP1; Refs. 28, 30). Protein-protein interaction of CIDEA with UCP1 has been demonstrated in ectopic expression studies by coimmunoprecipitation; it is postulated that Cidea acts to inhibit UCP1 uncoupling activity, thereby resulting in leanness of CIDEA null mice (28, 30). Studies (10, 18, 36) also indicate a role for CIDEA in human energy balance where CIDEA depletion in cultured human adipocytes has been demonstrated to stimulate lipolysis (36). CIDEB, which is highly expressed in liver, has recently been found to be an important regulator of lipid metabolism in liver (27). CIDEB-null mice evidence lower levels of plasma triglycerides and free fatty acids and are resistant to high-fat diet-induced obesity and liver steatosis; these mice also had increased insulin sensitivity, enhanced rates of whole body metabolism and hepatic fatty acid oxidation, and decreased lipogenesis (27). Thus CIDEs appear to be a family of proteins that have dual functions in apoptosis and in the physiology of normal healthy cells. Our studies herein provide new details on the regulation of the endogenous FSP27 transcript in the adipocyte lineage and in obesity and support the notion that FSP27 has a dual function(s) in adipocyte metabolism and in cellular apoptosis.

## MATERIALS AND METHODS

**Cell culture and adipocyte differentiation.** 3T3-L1 cells were obtained from American Type Culture Collection (Manassas, VA) and propagated in DMEM supplemented with 10% calf serum. For dif-

ferentiation, 3T3-L1 cells were treated at 2 days postconfluence with DMEM supplemented with 10% FCS in the presence of the adipogenic inducers 0.5 mM methylisobutylxanthine (MIX) and 1  $\mu$ M dexamethasone for 48 h. Adipogenic agents were then removed, and growth of cultures was continued in DMEM containing 10% FCS. At 5 days postinduction of differentiation, adipocyte conversion occurred in ~90% of the cells, as judged by lipid accumulation and cell morphology.

For differentiation of brown preadipocytes obtained from C. R. Kahn (Joslin Diabetes Foundation, Harvard Medical School, Boston, MA), cells were cultured to confluence in DMEM with 10% FCS, 20 nM insulin, and 1 nM triiodothyronine [differentiation medium per Klein et al. (24)]. Confluent cells were incubated in differentiation medium that was supplemented with 0.5 mM MIX, 0.5  $\mu$ M dexamethasone, and 0.125 mM indomethacin for 48 h. After this period, nearly 100% of cells showed adipogenic conversion at which time culture medium was replaced with differentiation medium and was replenished every 2 days thereafter.

For culture and differentiation of primary white adipocytes, WAT collected from male Sprague-Dawley rats was digested with 1 mg/ml of type I collagenase for 40 min with shaking at 37°C. After digestion, material was filtered through a 300- $\mu$ m pore size nylon mesh (Sefar America, Depew, NY) and filtrate centrifuged at 2,000 rpm for 5 min. The floating adipocyte fraction was removed, and the pellet of stromal-vascular cells was resuspended in DMEM containing 10% FCS and plated. Upon confluence cells were either harvested or subjected to differentiation media consisting of DMEM containing 10% FCS, 0.1  $\mu$ M dexamethasone, 0.25 mM MIX, and 17 nM insulin for 3 days at which time differentiation media were removed and cell cultures were maintained in DMEM containing 10% FCS and 17 nM insulin. Human preadipocyte and adipocyte RNA were purchased from Zen-Bio (Research Triangle Park, NC).

**TNF- $\alpha$ , insulin, and inhibitor treatment of 3T3-L1 adipocytes.** For treatments of 3T3-L1 adipocytes with TNF- $\alpha$ , cells were incubated with TNF- $\alpha$  for the indicated dose and times in DMEM supplemented with 10% FCS. For studies of regulation by insulin, 3T3-L1 adipocytes were cultured for 16 h in serum-free DMEM with 0.5% BSA and media were then changed to DMEM containing 0.5% BSA supplemented with insulin, as indicated. For studies using inhibitors to assess signaling mechanisms in 3T3-L1 adipocytes, cells were treated with 50  $\mu$ M PD-98059, 50  $\mu$ M LY-294002, or 1  $\mu$ M rapamycin (Sigma-Aldrich, St. Louis, MO), or DMSO vehicle. For inhibitor studies, in the case of TNF- $\alpha$ , experiments were carried out in normal serum-containing culture conditions with a 1-h pretreatment with the indicated inhibitor or with DMSO vehicle, followed by a 16-h culture with or without 10 ng/ml TNF- $\alpha$ . For studies of the effects of pharmacological inhibitors on insulin signaling, cells were first serum starved for 6 h, pretreated with inhibitor or DMSO vehicle for 1 h, and treated with 100 nM insulin or untreated for 16 h. Studies were carried out in either duplicate or triplicate in wholly independently conducted experiments.

**RNA preparation and transcript expression analysis.** For studies of transcript expression in murine tissues, 8-wk-old C57BL/6 or *ob/ob* male mice were used. All animal procedures were carried out with approval from University of Toledo Health Science Campus Animal Care and Use Committee. RNA was purified using TriZol reagent (Invitrogen) according to the manufacturer's instruction. For Northern blot analysis, 5  $\mu$ g of RNA were fractionated in 1% agarose-formaldehyde gels in MOPS buffer and transferred to Hybond-N membrane (GE Healthcare, Piscataway, NJ). <sup>32</sup>P-labeled probes for use in Northern blot analysis were synthesized using a random-priming kit (Promega). Blots were subject to 1-h hybridization in ExpressHyb solution (BD Biosciences Clontech, Palo Alto, CA). After high-stringency washing, membranes were exposed at -80°C to Kodak Biomax film with a Kodak Biomax intensifying screen or to a phosphorimager screen and read using a Typhoon 8600 PhosphorImager (GE Healthcare). In some instances blots were rehybridized with a probe for

36B4 transcript, which encodes the acidic ribosomal phosphoprotein PO, a commonly used internal control (26).

For real-time PCR, total RNA was isolated as above and subjected to DNase I treatment and cleanup (Qiagen). Reverse transcription was performed with SuperScript II RNase H-reverse transcriptase (Invitrogen) and an oligo(dT)-22 primer. Transcript levels were assessed by SYBR Green-based real-time PCR conducted with an ABI 7500 real-time PCR System (Applied Biosystems, Foster City, CA). Reaction conditions were  $1 \times$  SYBR Green PCR Master Mix (Applied Biosystems), 100 nM each forward and reverse primers, and 50 ng of cDNA. PCR was carried out over 40 cycles of 95°C for 15 s, 60°C for 30 s, and 72°C for 34 s with an initial cycle of 50°C for 2 min and 95°C for 10 min. Primers used were as follows: FSP27: 5'-CA-GAAGCCAATAAGAAGATCG-3' and 5'-TGTAGCAGTGCAG-GTCATAG-3'; and GAPDH: 5'-AACAGCCTCAAGATCATCAGC-3' and 5'-GGATGATGTTCTGGAGAGCC-3'. Expression was normalized against respective GAPDH transcript level and fold differences calculated. Statistical analyses were conducted on triplicates using single factor ANOVA.

**Cellular fractionation of adipose tissue.** To assess expression of FSP27 in adipose tissue components *in vivo*, tissue was fractionated into adipocyte and stromal vascular fractions. For this, WAT and BAT were removed from male C57BL/6 mice, rinsed three times in sterile PBS, and minced with scissors. Tissue was transferred to a 50-ml sterile tube with 15 ml of HBSS containing 0.2 mg/ml of type II collagenase (Sigma-Aldrich). After digestion for 40 min at 37°C with constant agitation, the material was filtered through a 300- $\mu$ m pore size nylon mesh. Filtrate was collected into sterile 50-ml centrifuge tubes and centrifuged at 2,000 rpm for 5 min. The floating adipocyte cell fraction was then lysed in 10 vol of TriZol reagent, and the stromal-vascular pellet fraction was lysed in 2 ml TriZol reagent. RNA was extracted and analyzed by Northern blot analysis as described in *RNA preparation and transcript expression analysis*.

**Constructs for mammalian expression.** Full-length expression constructs for murine (GenBank BC099676) and human FSP27 (GenBank BC016851) in the vector CMVSPORT6 were obtained as an I.M.A.G.E. clone from American Type Culture Collection, and the full sequence was verified. To prepare the HA-FSP27-FLAG expression construct, PCR amplification was carried with human FSP27 as template to amplify the open reading frame of FSP27. A FLAG epitope tag was incorporated into the 3'-PCR primer, and KpnI and BamHI restriction enzyme sites were incorporated, respectively, into the 5'- and 3'-PCR primer pairs to facilitate directional subcloning into an NH<sub>2</sub>-terminal epitope tag CMV expression vector (kindly provided by W. Maltese, University of Toledo Health Science Campus). For enhanced green fluorescent protein (EGFP) fusion protein studies, the open reading frame of human FSP27, minus the initiator methionine, was PCR amplified and subcloned into the pEGFP-C1 vector (Clontech), resulting in an expression construct wherein the EGFP protein is present NH<sub>2</sub> terminal to the FSP27 coding region. The inserts, cloning junctions, and epitope tag regions of all constructs were fully sequence verified.

**Cell death assay.** To assess the effects of ectopic expression of mFSP27 on cell viability, 293T cells or 3T3-L1 preadipocytes were cotransfected with an mFSP27 expression construct or empty vector in combination with a  $\beta$ -galactosidase (LacZ) expression construct. The mass of DNA(s) utilized is presented in the respective figure legend. Transfections were done in triplicate using Lipofectamine 2000 (Invitrogen), and the numbers of LacZ-transfected cells were assessed at 48 h posttransfection via  $\beta$ -galactosidase staining. For this, cells were fixed at room temperature in 0.5% glutaraldehyde. After two PBS washes, cells were incubated in staining solution [2 mM MgCl<sub>2</sub>, 5 mM K<sub>3</sub>Fe(CN)<sub>6</sub>, 5 mM K<sub>4</sub>Fe(CN)<sub>6</sub>, and 1 mg/ml 5-bromo-4-chloro-3-indolyl- $\beta$ -D-galactopyranoside in PBS] and incubated at 37°C for 4 h. After incubation, blue cells per microscopic field (200 $\times$ ) were enumerated with 10 independently and randomly chosen fields analyzed per transfection. This protocol has been used in previous studies of apoptosis (13) and was kindly provided by H. F. Ding

(University of Toledo Health Science Campus). This assay serves as an indirect and visual measurement of cell death. The  $\beta$ -galactosidase expression construct serves as a reporter to mark transfected cells, which are also cotransfected with a test "effector" plasmid, in this case FSP27 or an empty vector pcDNA3.1 control. Depending on the cell type under study, cells that have undergone cell death are lost from the cultures and are thus not counted among the LacZ<sup>+</sup> blue cells nor appear as very small round LacZ<sup>+</sup> blue apoptotic bodies. Comparison of the numbers of LacZ<sup>+</sup> blue cells in those cultures transfected with empty vector vs. those transfected with the "effector" plasmid (i.e., FSP27) allows for the detection of cell death attributable to the "effector" plasmid. Single-factor ANOVA was used for statistical assessments. Microscopic fields of cells in the studies were observed and photographed using an Olympus IX70 fluorescence microscope and Spot Advanced Software Version 4.9.0 (Diagnostic Instruments). All images shown accurately represent the original data; however, in some instances brightness and contrast were adjusted to allow for better visualization of details.

For DNA fragmentation assays, genomic DNA was prepared from 3T3-L1 preadipocytes, 3T3-L1 adipocytes, or transfected 293T cells. For the latter, 2  $\mu$ g of the murine FSP27 expression construct or empty vector were transfected in 293T cells using Lipofectamine 2000. DNA was prepared with an apoptotic DNA-ladder kit (Roche Diagnostics, Nutley, NJ) exactly per manufacturer's directions or by manual preparation using standard methods. For the latter, cells were collected from the media and culture plates and subjected to low speed centrifugation. The pellet was resuspended in cell lysis buffer (0.5% SDS, 20 mM EDTA, and 5 mM Tris·HCl pH 8.0), and lysates were incubated on ice for 20 min. Insoluble material was removed by centrifugation, and the supernatant was extracted with phenol/chloroform. DNA was ethanol precipitated, and the pellet was resuspended in water and subject to RNase digestion. DNA was assessed by fractionation on 1.2% agarose gels, stained, visualized under short-wave ultraviolet illumination, and photographed.

**Western blot analysis.** 293T cells were transfected with 2  $\mu$ g of FSP27 or empty vector and harvested at 48 h posttransfection by lysis in TNN(+) buffer (10 mM Tris pH 8.0, 120 mM NaCl, 0.5% NP-40, and 1 mM EDTA supplemented with a protease inhibitor cocktail). Lysates were incubated on ice for 30 min with intermittent vortexing, the supernatant was collected via centrifugation, and protein content was determined (Bio-Rad, Hercules, CA). For Western blot analysis, 30  $\mu$ g of protein extract were fractionated on SDS-PAGE, followed by electroblotting onto polyvinylidene difluoride membrane with 0.025 M Tris-0.192 M glycine transfer buffer supplemented with 20% methanol. Membranes were blocked for 1 h in 5% nonfat milk in PBS containing 0.5% Tween 20 (PBS-T) followed by either 1-h incubation at room temperature or overnight at 4°C, with a 1:2,000 dilution of antibody to full-length poly-ADP-ribose polymerase (PARP; Affinity BioReagents) or cleaved PARP,  $\alpha$ -fodrin, cleaved  $\alpha$ -fodrin (Cell Signaling Technology), or a 1:10,000 dilution of  $\beta$ -tubulin (Covance Research Products). Polyclonal FSP27 antibody was used at 1:1,000 and was produced by arrangement with ProSci, using a full-length mouse FSP27-TrpE fusion protein as immunogen. Secondary antibody was HRP-conjugated goat anti-rabbit (Bio-Rad) and used at a 1:2,000 dilution, and washes were conducted in PBS-T. Signal was detected by ECL Plus enhanced chemiluminescence (GE Healthcare) and exposure to X-ray film.

**Localization studies.** Confocal imaging studies using MitoTracker Red CMX Ros (Invitrogen) were conducted on live cells by plating 3T3-L1 preadipocytes or COS cells onto laminin-coated MatTek glass bottom dishes (MatTek, Ashland, MA) at a density of  $3 \times 10^5$  cells per 35-mm diameter dish. For studies using DSRed2-Mito (Clontech), COS cells were plated onto laminin-coated coverslips and observed after methanol fixation. Cells were transfected using Lipofectamine 2000 with 2  $\mu$ g of either EGFP empty vector or EGFP-FSP27 construct (for MitoTracker studies) or with 1  $\mu$ g of EGFP empty vector or EGFP-FSP27 construct in combination with 1  $\mu$ g of pDSRed2-

Mito expression construct (Clontech). MitoTracker staining was used according to the manufacturer's instruction at a concentration of 50 nM for 45 min at 37°C. Cells were observed at ~20 h posttransfection. Confocal studies were performed using the resources of the Advanced Microscopy and Imaging Center at the University of Toledo Health Science Campus. Images were captured using a Leica TCS SP5 broadband confocal microscope (Leica, Mannheim, Germany) equipped with Argon-488 and diode-pumped solid-state-561 laser sources and 63.0 × 1.40 N.A. oil immersion objective. A series of optical Z sections, 0.5 μM in thickness and totaling 5–6 μM, were collected and visualized as projection images using Leica LAS software. Laser intensities and microscope settings between samples were maintained constant.

In the case of 3T3-L1 preadipocytes transfected with either EGFP empty vector or EGFP-FSP27 construct and used for observation of apoptotic morphology, cells were plated at a density of  $5 \times 10^4$  per well of six-well plates. Nuclei of live cells were stained at 24 h posttransfection with 1 μg/ml Hoechst dye for 20 min at 37°C and observed and photographed using an Olympus IX70 fluorescence microscope and Spot Advanced Software version 4.9.0. All images shown accurately represent the original data; however, in some instances, brightness and contrast were adjusted to allow for better visualization of details.

## RESULTS

*Differentiation-dependent expression of FSP27 in multiple models of adipogenesis.* Despite the fact that Danesch et al. (11) initially identified FSP27 over two decades ago, information on the expression and regulation of the endogenous FSP27 transcript is minimal. FSP27 was originally identified as a transcript upregulated during in vitro adipose conversion of TA1 cells (11). They also demonstrated that a 2.5-kb fragment of the FSP27 promoter evidenced adipocyte differentiation-dependent expression. This was ascribed in part to functional CEBPα binding sites in the FSP27 promoter, although the direct transcriptional activation of the FSP27 promoter by CEBPα was not investigated (11). TA1 cells are a rarely utilized preadipocyte cell line established by Chapman et al. (7, 25) via treatment of the murine 10T1/2 mouse embryo fibroblast cell line with the demethylating agent 5-azacytidine; this model system for in vitro adipogenesis was used solely by Chapman et al. (6). TA1 cells are, therefore, not well characterized, in contrast to the many key molecular events of adipogenesis that have been delineated in the 3T3-L1 in vitro adipogenesis model. Thus we deemed it important to define the expression of the FSP27 transcript in the widely used and well-characterized 3T3-L1 model. As shown by the Northern blot analysis in Fig. 1A, the FSP27 transcript is not detected in 3T3-L1 preadipocytes and is readily detected starting at 2 days postinduction and continues to increase throughout the 5-day time point, which represents mature 3T3-L1 adipocytes. Real-time PCR analysis indicated a  $5.7 \times 10^4$ -fold increase ( $P < 0.001$ ) in the FSP27 transcript level in day 7 adipocytes vs. preadipocytes. Adipocyte conversion is validated by expression of the adipocyte marker genes stearoyl Co-A desaturase 1 (SCD1), adipocyte fatty acid binding protein (aFABP), adipose tissue triglyceride lipase (ATGL), and PPARγ.

We next examined expression of the FSP27 transcript in several additional models of adipogenesis. We found that the FSP27 transcript is not detected in rat primary preadipocytes and that expression of the FSP27 transcript emerges upon their adipocyte conversion (Fig. 1B), paralleling that of the adipocyte

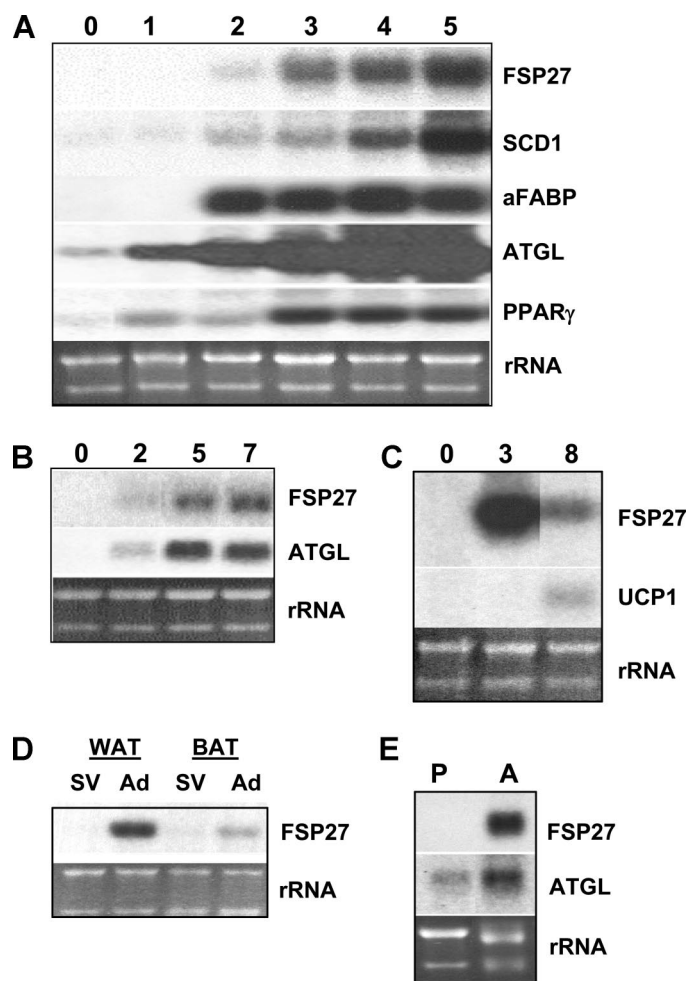


Fig. 1. Northern blot assessment of the fat-specific protein 27 (FSP27) transcript upregulation in multiple adipogenesis models. *A*: 3T3-L1 cells. RNA was harvested from 3T3-L1 preadipocytes (day 0) and at daily intervals through day 5 postinduction of adipogenesis. *B*: rat primary cultures. Primary cultures of rat preadipocytes were harvested for RNA preparation at days 0 and at days 2, 5, and 7 postadipogenic induction. *C*: murine brown preadipocytes. RNA was harvested from cultures as preadipocytes at day 0 and at days 3 and 8 postinduction of adipogenesis. *D*: in vivo adipose tissue fractions. RNA was harvested from stromal-vascular (SV) fraction or adipocyte (Ad) fraction cell populations prepared from C57BL/6 murine white adipose tissue (WAT) and brown adipose tissue (BAT). *E*: analysis of primary human preadipocytes (P) and from in vitro differentiated human adipocytes (A). For each of the above, Northern blot analysis was performed on 5 μg total RNA with indicated random-primed  $^{32}$ P-labeled probes and ethidium bromide (EtBr) staining of rRNA is shown below autoradiogram. For *A*, *B*, and *C*, numbers above lanes indicate days. In the case of *A*–*E*, all data shown in each row of boxed panel were obtained from the same original Northern blot; however, some data lanes were either removed or rearranged for economy and/or clarity of presentation. SCD1, stearoyl Co-A desaturase 1; aFABP, adipocyte fatty acid binding protein; ATGL, adipose tissue triglyceride lipase; PPARγ, peroxisome proliferator-activated receptor-γ.

cyte marker transcript ATGL. The regulation of expression of FSP27 during brown adipogenesis is unknown, although we (see Fig. 6) and others (64) have detected its expression in BAT. To examine this, we used a permanent brown preadipocyte cell line established by Klein et al. (24) that was derived from neonatal BAT. In this cell culture model, brown adipocyte conversion is evidenced by emergence of the brown adipocyte-specific transcript UCP1 and by multilocular lipid

accumulation and cell morphology (data not shown). As shown in Fig. 1C, the FSP27 transcript is not found in brown preadipocytes and is detected at both 3 and 8 days postinduction of adipocyte conversion, with a particularly enriched signal found at day 3. Quantitation of FSP27 in brown preadipocytes (day 0) and brown adipocytes (day 8) by real-time PCR indicated a 57-fold increase ( $P < 0.001$ ) in the FSP27 transcript level during brown adipogenesis. We also determined expression of FSP27 in adipose tissue cell types derived from an in vivo source. For this whole murine, WAT and BAT were fractionated into adipocytes and the nonadipocyte stromal-vascular fraction. Figure 1D indicates that the FSP27 transcript is not detected in stromal-vascular cells, which are the source of in vivo preadipocytes, but is readily detected in the adipocyte cell population of WAT and BAT. We also addressed adipocyte differentiation dependent expression of the FSP27 transcript in in vitro differentiation of primary human preadipocytes. Figure 1E shows that while the FSP27 transcript is not detected in human preadipocytes it is readily detected in differentiated human adipocytes. Thus by assessing multiple adipocyte model systems, we conclude that upregulation of the FSP27 transcript is integral to the molecular definition of white and brown adipocytes. Puri et al. (39) recently indicated a similar adipocyte enriched expression for the FSP27 transcript, although in that case the data were not shown. The full regulatory pathways governing adipocyte expression of FSP27 are not currently known. However, as discussed above, CEBP $\alpha$  action is implicated in that it has been demonstrated to physically bind at FSP27 promoter elements (11). At the time that FSP27 was under study by Danesch et al. (11) PPAR $\gamma$  had yet to be discovered. However, a microarray profiling study of a PPAR $\gamma$ 1 transgenic mouse model indicates FSP27 might also be a target of PPAR $\gamma$  transactivation. These mice were found (63) to express elevated levels of a number of adipocyte transcripts in liver, including FSP27.

*TNF- $\alpha$  downregulates the FSP27 transcript in 3T3-L1 adipocytes.* A previous study (59) indicated that downregulation of an FSP27 promoter-CAT reporter construct occurred at 3 h of TNF- $\alpha$  treatment of TA1 adipocytes, and this was ascribed as likely due to TNF- $\alpha$ -mediated downregulation of CEBP $\alpha$ . However, we are not aware of reports on the regulation of the endogenous FSP27 transcript level by exogenous agents such as cytokines or hormones. As our ultimate goal is to fully understand the regulation and function of FSP27 in the adipocyte lineage, we assessed the regulation of the FSP27 transcript in 3T3-L1 adipocytes by treatment with insulin and TNF- $\alpha$ , two agents closely linked to normal adipocyte metabolism and adipocyte pathophysiology. Comprehensive oligonucleotide microarray assessments of the global transcriptional response of 3T3-L1 adipocytes to TNF- $\alpha$  have revealed that this cytokine has global effects on 3T3-L1 adipocyte gene expression (47, 48). It has long been known that TNF- $\alpha$  treatment of preadipocytes inhibits adipogenic conversion (54, 62) and exposure of adipocytes to TNF- $\alpha$  stimulates lipolysis (53) and promotes a dedifferentiated adipocyte phenotype (62). These effects have been ascribed, at least in part, to the TNF- $\alpha$ -mediated transcriptional downregulation of the master adipocyte transcription factor PPAR $\gamma$  (62) and CEBP $\alpha$  (59).

Figure 2A reveals the regulation of the FSP27 transcript with a 24-h exposure of 3T3-L1 adipocytes to a range of TNF- $\alpha$  concentrations. These studies were conducted in FCS-contain-

ing media, culture conditions typically used to demonstrate the TNF- $\alpha$ -mediated effects adipocyte dedifferentiation of 3T3-L1 cells. TNF- $\alpha$  treatment was highly effective at downregulating the FSP27 transcript level and did so at the lowest TNF- $\alpha$  concentration tested (0.01 ng/ml). It was similarly effective 10 ng/ml, a concentration that is typically used for studies of TNF- $\alpha$  effects in adipocytes; real-time PCR revealed that this treatment reduced the FSP27 transcript to  $\sim 12\%$  of the level in control untreated cells ( $P < 0.001$ ). Also shown is the effect of TNF- $\alpha$  on three other adipocyte-enriched genes, ATGL, resistin, and SCD1. Here, distinctions are noted in the concentration-dependent decrease among these transcripts in that the 0.01 ng/ml treatment effectively reduced FSP27 and resistin transcript levels but was largely ineffective in regard to transcripts for ATGL and SCD1. Figure 2B shows a Northern blot analysis for temporal assessment of FSP27 transcript levels in untreated 3T3-L1 adipocytes (0 h) through 48 h of 10 ng/ml TNF- $\alpha$  treatment. A reduction of the FSP27 transcript level is clearly noted at 4 h of TNF- $\alpha$  exposure; this decrease is sustained through the final time point examined (48 h). Real-

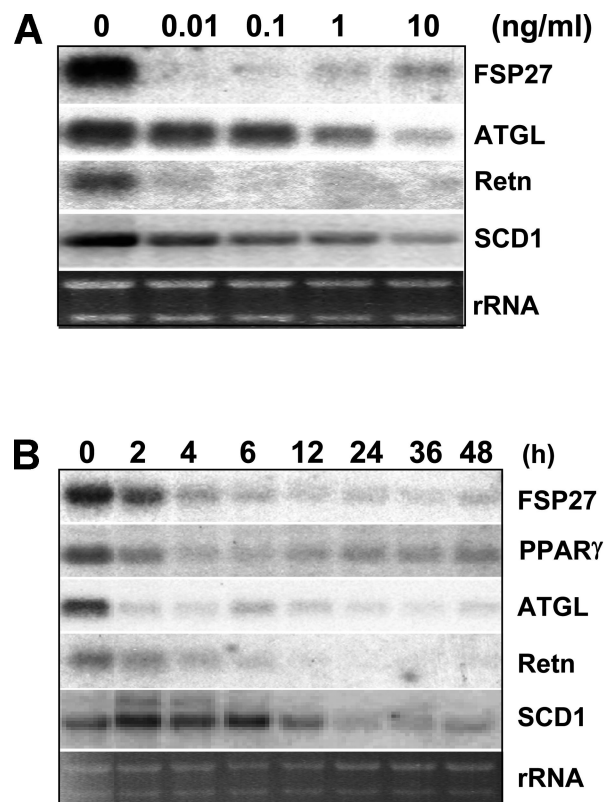


Fig. 2. Concentration and temporal effects of TNF- $\alpha$  on FSP27 and select adipocyte-enriched transcripts in 3T3-L1 adipocytes. *A*: 3T3-L1 adipocytes were treated with the indicated concentration of TNF- $\alpha$  for 24 h and FSP27, ATGL, resistin (Retn), and SCD1 transcript levels were analyzed by Northern blot using random-primed  $^{32}\text{P}$ -labeled probes. *B*: 3T3-L1 adipocytes were treated with 10 ng/ml of TNF- $\alpha$  for indicated time points. Five micrograms of total RNA were analyzed by Northern blot using random-primed  $^{32}\text{P}$ -labeled probes for FSP27, PPAR $\gamma$ , ATGL, Retn, and SCD1 probes. EtBr staining of rRNA, shown below autoradiogram, was used to assess gel loading. Dose-response and time-course studies were conducted in duplicate and representative data shown. In the case of *A* and *B*, all data shown in each row of boxed panel were obtained from same original Northern blot; however, some data lanes were either removed or rearranged for economy and/or clarity of presentation.

time PCR analysis indicated that TNF- $\alpha$  treatment reduced FSP27 to 10% of that in control cells ( $P < 0.001$ ) when measured at the 24-h time point. The temporal effects of TNF- $\alpha$  on the FSP27 transcript level are similar to that for the master adipogenic transcriptional regulator PPAR $\gamma$  and for two of the three other adipocyte-enriched genes we assessed, ATGL and resistin. A third adipocyte-enriched transcript, SCD1, also evidences downregulation by the TNF- $\alpha$ , albeit with a somewhat slower temporal effect.

To investigate the intracellular signaling pathways underlying downregulation of the FSP27 transcript by TNF- $\alpha$ , we pretreated 3T3-L1 adipocytes with specific pharmacological inhibitors and assessed the FSP27 transcript level in the absence or presence of TNF- $\alpha$ . The results are shown in the Northern blot analysis in Fig. 3A and the accompanying graphical representation in Fig. 3B. Neither a pretreatment with the p44/42 MAP kinase inhibitor PD-98059 nor the p70S6 kinase inhibitor rapamycin affected levels of the endogenous FSP27 transcript, nor did either of these inhibitors attenuate the TNF- $\alpha$ -mediated decrease of the FSP27 transcript level. In the case of LY-294002, a phosphatidylinositol 3-kinase (PI3-kinase) inhibitor, treatment with this inhibitor alone resulted in a dramatic reduction of the FSP27 transcript level to 15% of the level of the DMSO vehicle-treated control. The regulation of endogenous FSP27 we note upon treatment with LY-294002 alone makes an assessment of its effect in the presence of TNF- $\alpha$  difficult to ascertain. However, LY-294002 did not block the effects of TNF- $\alpha$  on the FSP27 transcript level and, if anything, resulted in a small additional inhibition. Moreover, the observation that LY-294002 alone led to a marked reduction of the endogenous FSP27 transcript in serum-containing culture conditions suggested that a component of FCS, the signaling mechanism of which is affected by LY-294002, was responsible for the noted attenuation of expression of the FSP27 transcript level.

*FSP27 transcript level is under tight regulation by insulin and involves PI3-kinase signals.* To specifically address the ability of insulin to regulate the FSP27 transcript, we utilized in vitro studies with 3T3-L1 adipocytes. Given that serum components might interfere with our assessments, these studies were carried out in serum-free conditions. Figure 4A shows the Northern blot analysis for the FSP27 transcript under culture conditions of no insulin through 200 nM insulin. An increase in the FSP27 transcript level is observed at the lowest insulin concentration tested (0.1 nM) with a similar magnitude of increase noted for each of the insulin concentrations tested. The Northern blot in Fig. 4B reveals the temporal nature of the response and indicates that insulin markedly increases the FSP27 transcript level within 24 h, while no change in the FSP27 transcript was evident in time-matched serum-free cultures.

We next addressed the mode of insulin action in upregulation of the FSP27 transcript by pretreatment with DMSO (vehicle), PD-98059, LY-294002, or rapamycin. For these studies, 3T3-L1 adipocytes were cultured under serum-free conditions with the indicated inhibitors only or cultured with insulin in the presence of the indicated inhibitors. As shown by the Northern blot analysis and the accompanying graphical representation of this data (Fig. 5, A and B), a barely detected signal for the FSP27 transcript was found under serum-free culture conditions in the absence exogenous insulin. Insulin

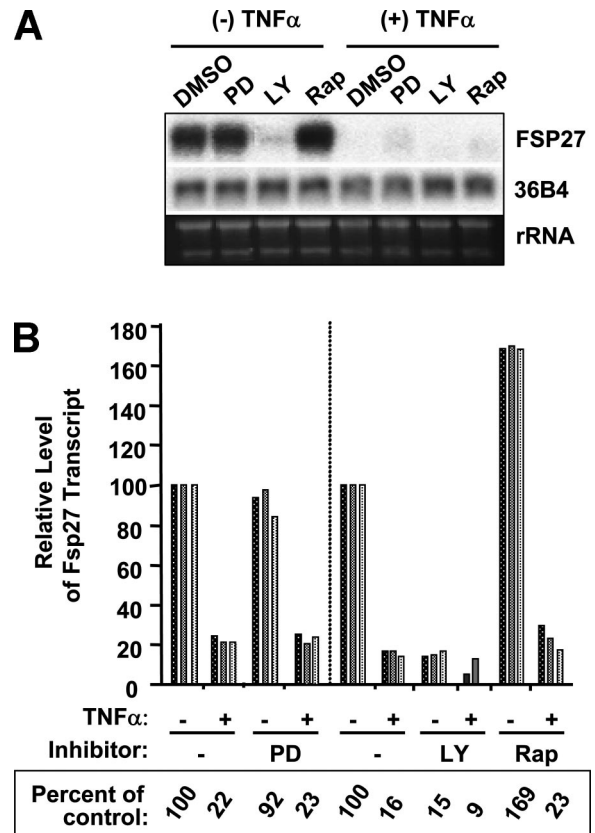


Fig. 3. Intracellular signaling pathways involved in TNF- $\alpha$ -mediated downregulation of the FSP27 transcript in 3T3-L1 adipocytes. *A*: 3T3-L1 adipocytes were pretreated for 1 h with DMSO vehicle, PD-98059 (PD, 50  $\mu$ M), LY-294002 (LY, 50  $\mu$ M), and rapamycin (Rap, 1  $\mu$ M) before addition of 10 ng/ml TNF- $\alpha$  for 16 h or without TNF- $\alpha$  addition. RNA was analyzed for FSP27 and 36B4 transcripts by Northern blot using random-primed  $^{32}$ P-labeled probes. EtBr staining of rRNA is shown below autoradiogram. Data shown in each row of boxed panel was obtained from same original Northern blot; however, some data lanes were either removed or rearranged for economy and/or clarity of presentation. The experiment was carried out 2 times, and representative data are shown. *B*: graphical representation of the response of the FSP27 transcript to pharmacological inhibitors of intracellular signaling. Northern blot analyses were conducted as in *A* and FSP27 transcript level for each sample normalized against its 36B4 control by phosphorimager analysis to correct for variations in sample loading. Numbers shown below graph are average change in FSP27 transcript level per treatment group, expressed as percentage of value for DMSO vehicle control untreated with TNF- $\alpha$ . Data are from triplicate studies conducted studies (represented by dark, medium, and light gray shaded bars); however, one of the +TNF- $\alpha$ /+LY was lost in processing. Vertical dashed line demarcates data from 2 wholly separate studies with indicated inhibitors, either for effects of PD treatment (left of line) or for effects of LY and Rap treatment (right of line); as such left and right regions of graph each have their own respective control values. Data in *A* and *B* derive from wholly distinct sets of studies.

stimulated the FSP27 transcript level by approximately eight-fold over that of DMSO vehicle-treated control cultures. The magnitude of this increase was not affected by PD-98059 or rapamycin pretreatment. That these two agents were unable to block the insulin upregulation of the FSP27 transcript suggests that neither p44/42 MAP kinase nor p70S6 kinase signals function in the insulin responsiveness of the FSP27 gene. In marked contrast, pretreatment of adipocytes with LY-294002 reduced the magnitude of the insulin stimulation of the FSP27 transcript level to 14% of that of insulin-treated control cultures. We were concerned that the barely detectable level of the

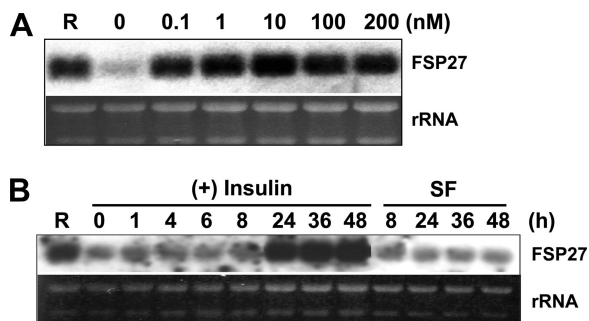


Fig. 4. Concentration and temporal effects of insulin on the FSP27 transcript level in 3T3-L1 adipocytes. **A:** 3T3-L1 adipocytes were incubated in serum-free medium for 16 h (*time 0*) or in regular growth media (R) at which time serum-free cultures were further incubated with the indicated concentration of insulin for 36 h. EtBr staining of rRNA, shown below autoradiogram, was used to assess gel loading. **B:** 3T3-L1 adipocytes were incubated in serum-free medium for 16 h (designated as 0) or in regular serum-containing growth media, at which time serum-free cultures were further incubated for the indicated times in the presence of 100 nM insulin [(+)insulin] or in its absence (SF). Northern blot hybridization was conducted using random-primed  $^{32}\text{P}$ -labeled probe for FSP27. EtBr staining of rRNA, shown below autoradiogram, was used to assess gel loading. Dose-response and time-course studies were carried out 2 times, and representative data are shown. All data shown in each row of single boxed panel were obtained from same original image of a Northern blot; however, in the case of **B** data lanes were either removed or rearranged for economy and/or clarity of presentation.

FSP27 transcript present in serum-free insulin-free conditions may have limited our ability to assess the effects of inhibitors alone on the FSP27 transcript by quantitative Northern blot. However, real-time PCR analysis of the effects of LY-294002 under these conditions indicated that LY-294002 resulted in an 80% decrease in FSP27 transcript levels ( $P < 0.001$ ), similar to the 88% decrease found by quantitative Northern blot analysis. Together, these observations demonstrate that insulin stimulation of FSP27 transcript expression involves PI3-kinase, an intracellular mediator whose role in insulin signal transduction is well established.

**Expression of FSP27 in wild-type and obese murine tissues.** We next examined the tissue distribution of the FSP27 transcript in a wide panel of murine tissues by Northern blot analysis. Figure 6A demonstrates that the FSP27 transcript is highly enriched in murine WAT and also demonstrates readily detectable expression in BAT. Adipose tissue enrichment of FSP27 was also recently confirmed by others, although the data for such was not shown (39). Also shown in Fig. 6A is the murine tissue distribution for the other two CIDE family members. As previously reported, CIDEA is highly enriched in murine BAT. In regard to murine CIDEB, we detect expression in liver as has been previously reported for the human transcript (20) and also demonstrate expression of CIDEB in murine intestine and kidney. Figure 6B shows assessment of the FSP27 transcript level in various murine tissues by real-time PCR and indicates that WAT expresses  $\sim 7.5$ -fold higher levels ( $P < 0.001$ ) than does BAT. Signal is also detected in several other tissues, albeit at a level  $>50$ -fold below ( $P < 0.001$ ) that found in WAT. In contrast to the fat-specific nature of FSP27 transcript expression in mice, very limited studies to date on the cell and tissue expression of human FSP27 have led to the suggestion that it is not particularly restricted to human adipose tissue (29).

We next addressed if the FSP27 transcript showed dysregulated expression in obese tissues using the murine *ob/ob* obesity model; such mice are obese due a mutation in the leptin gene. The Northern blot analysis in Fig. 7A indicates that WAT from wild-type and *ob/ob* mice show a similar level of the FSP27 transcript. However, upon examination of liver of wild-type and *ob/ob* mice for the FSP27 transcript, a dramatic increase was found for *ob/ob* liver (Fig. 7B). Real-time PCR analysis revealed a 49-fold enrichment ( $P < 0.001$ ) in liver of *ob/ob* mice, compared with wild-type C57BL/6 mice. The only data of which we are aware that may link FSP27 to liver

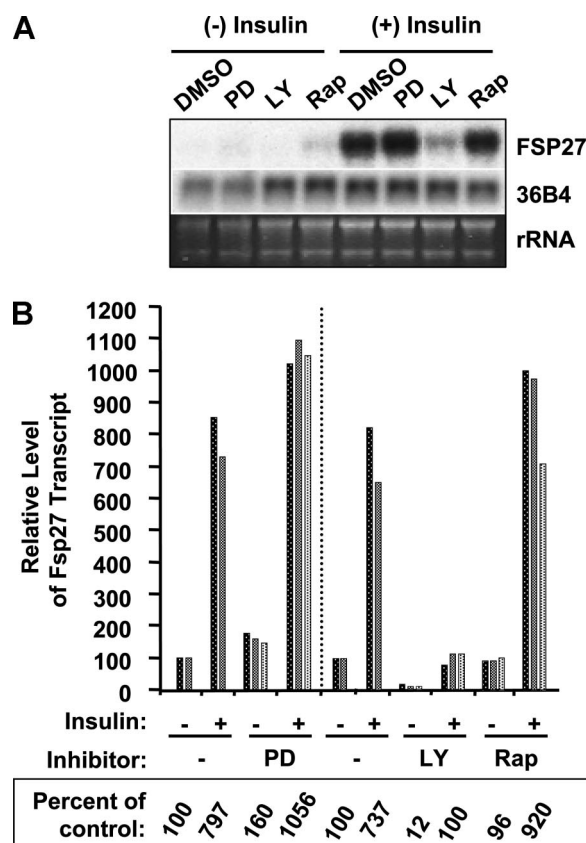


Fig. 5. Intracellular signaling pathways involved in insulin-mediated increase of the FSP27 transcript level in 3T3-L1 adipocytes. **A:** 3T3-L1 adipocytes were serum starved for 6 h and pretreated for 1 h with DMSO vehicle, PD-98059 (PD; 50  $\mu\text{M}$ ), LY-294002 (LY; 50  $\mu\text{M}$ ), and rapamycin (Rap; 1  $\mu\text{M}$ ), at which time they were subject to continued incubation under these conditions, in either the presence or absence of 100 nM insulin for an additional 16 h. Five micrograms of total RNA were analyzed by Northern blot for FSP27 and 36B4 transcript using random-primed  $^{32}\text{P}$ -labeled probes. EtBr staining of rRNA is shown below autoradiogram. All data shown in each row of single boxed panel was obtained from same original image of a Northern blot; however, some data lanes were either removed or rearranged for economy and/or clarity of presentation. The experiment was carried out 2 times, and representative data are shown. **B:** FSP27 transcript expression level was quantitated as described for Fig. 3. Numbers shown below graph are average change in the FSP27 transcript level per treatment group, expressed as percentage of value for DMSO vehicle control untreated with insulin. Data are from 3 independently conducted studies (represented by dark, medium, and light gray shadings); however, 1 of the (+)insulin and 1 of the (-)insulin samples was lost in processing. Vertical dashed line demarcates data from 2 wholly separate studies with the indicated inhibitors, either for effects of PD treatment (*left* of line) or for effects of LY and Rap treatment (*right* of line), as such *left* and *right* regions of graph each have their own respective control values. Data in **A** and **B** derive from wholly distinct sets of studies.

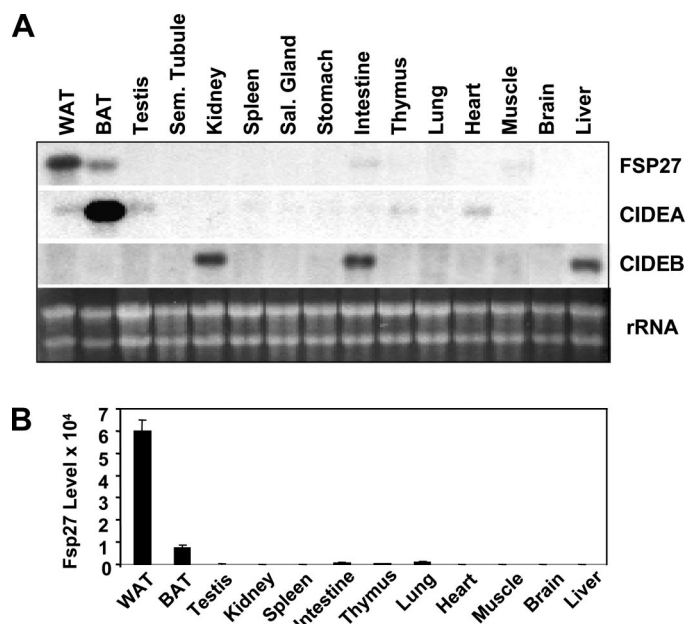


Fig. 6. Expression of the FSP27 transcript in wild-type murine tissues. **A**: Northern blot analysis was conducted on indicated tissues using random-primed <sup>32</sup>P-labeled probes for FSP27, cell death-inducing DFF45-like effector a (CIDEA), and CIDEB. All data shown in each row of boxed panel were obtained from the same original image of a Northern blot; however, some data lanes were either removed or rearranged for economy and/or clarity of presentation. **B**: real-time PCR analysis of expression of FSP27 in murine tissues. Sem. tubule, seminiferous tubule; Sal. gland, salivary gland.

dysfunction are a study by Yu et al. (63) on adipocyte-specific gene expression and adipogenic hepatic steatosis in the mouse liver due to PPAR $\gamma$ 1 overexpression on a PPAR $\alpha$  null background. Upregulation of a number of adipocyte enriched genes occurred in liver of these mice with an 11-fold increase reported for the FSP27 transcript (63). At this time, however, it is not possible to define the distinctions between the effects of upregulation of FSP27 and hepatic steatosis and the effects of the myriad of other genes also increased in the liver of these transgenic mice. We also detected upregulation of CIDEA transcript in *ob/ob* liver (Fig. 7C). No difference in FSP27 or CIDEA transcript level was detected for wild-type vs. *ob/ob* kidney, nor did we detect CIDEA in either wild-type or *ob/ob* adipose tissue (data not shown). The upregulation of CIDEA in *ob/ob* liver is in line with the finding by Kelder et al. (22) of enhanced expression of CIDEA in the liver of aged or type 2 diabetic mice exhibiting steatosis. It has also been reported that CIDEA is markedly induced in liver via activation of PPAR $\gamma$  and PPAR $\alpha$  transcription factors, which interact with their cognate PPREs in the CIDEA 5'-flanking region (58).

*Murine FSP27 is proapoptotic and leads to cleavage of PARP and  $\alpha$ -fodrin.* While human FSP27 has been determined to promote apoptosis upon ectopic expression in 293T and CHO cells, as evidenced by cell death and DNA fragmentation (29), to our knowledge murine FSP27 has not been examined for apoptotic effects. We thus first assessed the ability of murine FSP27 to promote apoptosis in 293T cells, a frequently used cell line for apoptosis studies. Figure 8A shows the result of a DNA fragmentation assay where DNA laddering is evident in FSP27-transfected cells at 18, 21, 24, and 48 h posttransfection compared with lack of detectable DNA laddering for

empty vector transfectants at the 48-h time point. This demonstrates for the first time that, as has been reported for human FSP27, that murine FSP27 is a proapoptotic molecule. As far as we are aware, apoptotic end points other than cell death and DNA fragmentation have not been described in regard to human FSP27 or murine FSP27 action. We therefore used Western blot analysis to examine whether apoptosis mediated by murine FSP27 resulted in the appearance of the cleaved forms of PARP and  $\alpha$ -fodrin, two well-described proteins that are targets for caspase-mediated cleavage during the apoptotic cascade. Figure 8B shows, for the first time, that FSP27 apoptosis leads to generation of cleaved PARP and  $\alpha$ -fodrin, which are present at 15 h and later time points, whereas minimal cleavage product(s) is present in empty vector transfectants. Given that PARP and  $\alpha$ -fodrin are targets for caspase-mediated cleavage, these data suggest that the proapoptotic effects of FSP27 are exerted, at least in part, through caspase-dependent mechanism(s). We also examined the time and dose response of cell death using an assay wherein transfected cells are marked blue due to cotransfection of a LacZ expression construct along with either empty vector or a murine FSP27 expression construct. As described in MATERIALS AND METHODS, in this assay loss of blue cells from the culture serves as an indirect indicator of cell death. Samples were collected for assessment of cell death at indicated time points posttransfec-

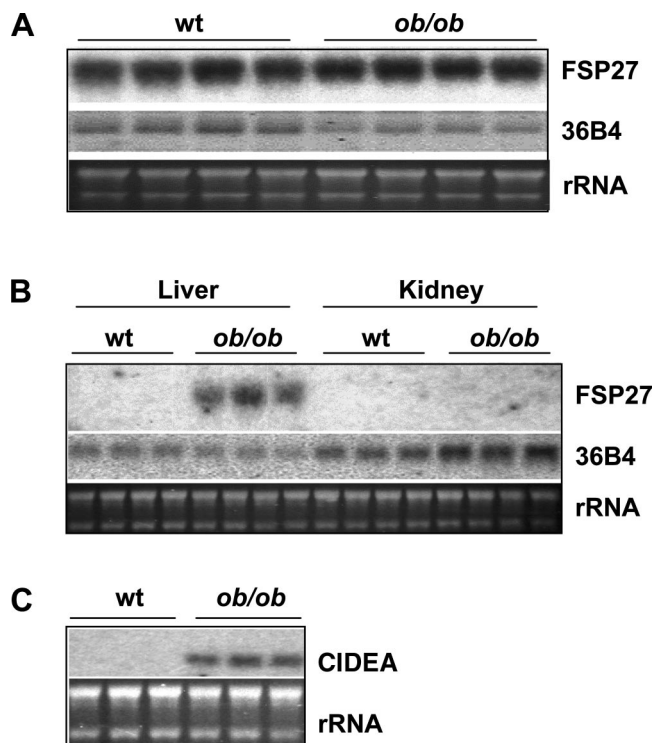
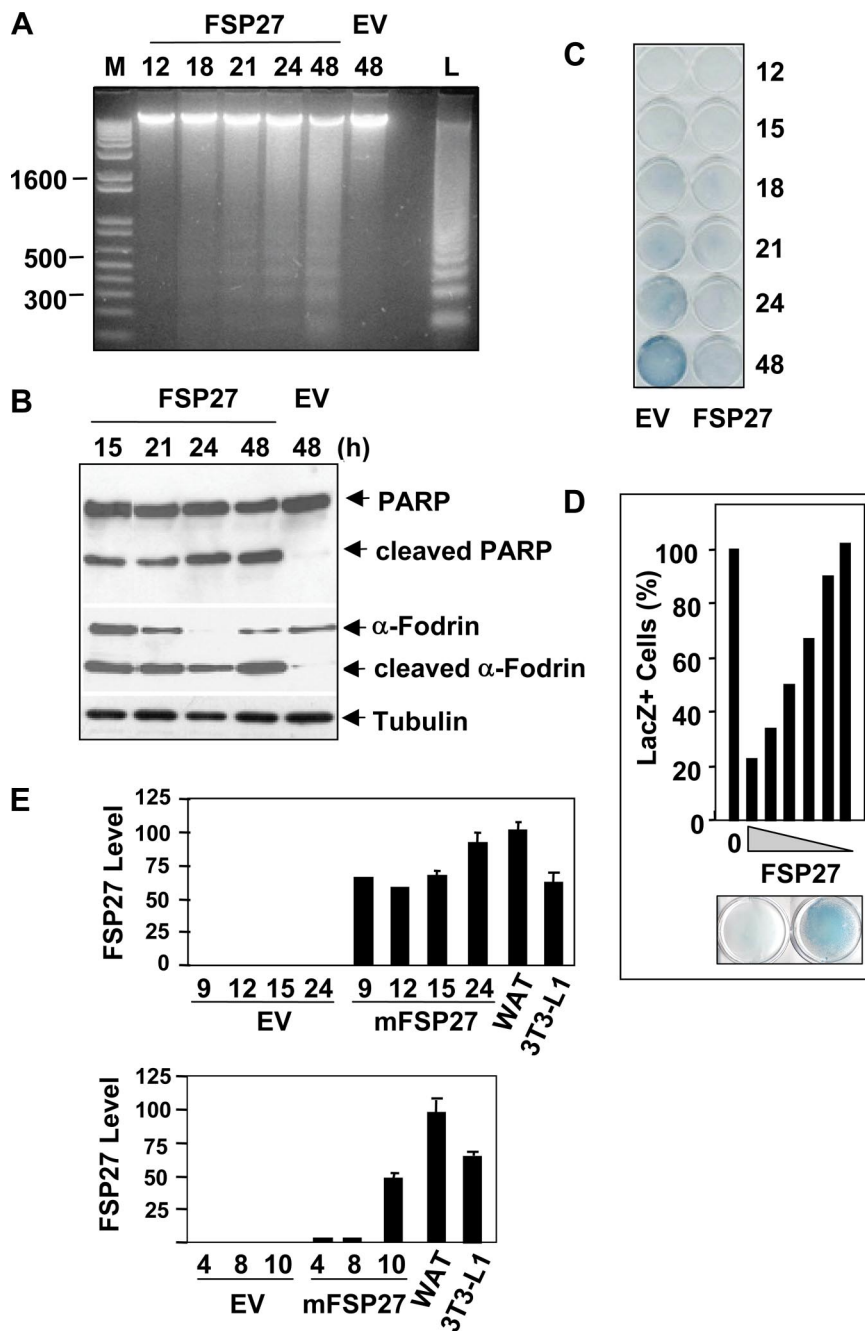


Fig. 7. Expression of the FSP27 transcript in *ob/ob* murine tissues. **A**: wild-type C57BL/6 (wt) and obese (*ob/ob*) WAT. Level of the FSP27 transcript in subcutaneous WAT (**A**), or liver and kidney (**B**), or of Cidea in liver (**C**), was assessed in individual wild-type and *ob/ob* mice by Northern blot analysis. EtBr staining of rRNA is shown below the respective autoradiogram. For **B** and **C**, blots were rehybridized to 36B4 as an internal control. Separate lanes represent tissue from different individual mice, with a minimum of 3 mice per genotype. All data shown in each row of the boxed panels were obtained from the same original image of a Northern blot; however, some data lanes were either removed or rearranged for economy and/or clarity of presentation.

Fig. 8. Apoptosis induced by murine FSP27 results in cleavage of PARP and  $\alpha$ -fodrin. **A:** genomic DNA was prepared and analyzed for fragmentation. A control apoptotic ladder (L) is shown at *right* and DNA marker (M) is shown in far *left* lane. **B:** 293T cells were transfected with 2  $\mu$ g FSP27 expression construct or empty vector (EV) and total protein was harvested at indicated time points posttransfection. Protein was subjected to SDS-PAGE and analyzed by Western blot for full-length and cleaved PARP, for full-length and cleaved  $\alpha$ -fodrin, and for  $\beta$ -tubulin. **C:** time course of FSP27-induced cell death. 293T cells were cotransfected with 0.1  $\mu$ g of a LacZ expression construct and either 1.90  $\mu$ g of EV or an FSP27 expression construct. At indicated hours posttransfection, cells were fixed and stained for  $\beta$ -galactosidase activity. Representative stained culture dishes are shown, where blue color indicates LacZ positive cells. **D:** dose response of FSP27-mediated cell death. 293T cells were transfected with an expression construct for murine FSP27 or EV and a LacZ expression construct. A total of 2  $\mu$ g of DNA was used per transfection comprised of 0.01  $\mu$ g of a LacZ expression construct and either EV (0) or an FSP27 expression construct, where the amount of FSP27 plasmid (2nd column) is 2  $\mu$ g, and the 5 subsequent columns to *right* represent transfections using decreasing mass of FSP27 expression that are 1/2, 1/4, 1/8, 1/16, and 1/32 of 2  $\mu$ g. At 48 h posttransfection, blue cells were enumerated as described in MATERIALS AND METHODS and expressed as percentage of EV transfectants (set at 100%). Data are average value of duplicate transfections. Images of culture dishes below graph are for 2  $\mu$ g transfection (*left*) and EV transfection (*right*). **E:** level of FSP27 transcript in transfected 293T cells compared with adipocytes. Real-time PCR was carried out on total RNA of 293T cells transfected with EV or with the mouse FSP27 expression construct and harvested at indicated times (in hours) posttransfection. A longer-term study is shown at *top*, and a shorter-term study at *bottom*. For *top*, the level in 9-h EV sample was set to a value of 1. For *bottom*, level in 4-h EV sample was set to a value of 1. Plotted data are FSP27 transcript level after correction for transfection efficiency of 293T cell population and percentage of adipocytes in either whole WAT (WAT) or differentiated 3T3-L1 (3T3-L1) cell populations, as described in text. In the case of A and B, all data shown in each single inclusive panel were obtained from the same original image of an agarose gel (A) or Western blot exposure (B); however, some data lanes were either removed or rearranged for economy and/or clarity of presentation.



tion and reveal that the proapoptotic effect of FSP27 can be clearly seen with the naked eye at 48 h, and microscopic evaluation showed a clearly discernable effect at 18 h (Fig. 8C, and data not shown). Figure 8D illustrates the dose response of cell death wherein a maximum of ~80% cell death is observed at the highest mass of FSP27 plasmid tested, and cell death diminishes with transfection of decreasing mass of the FSP27 expression construct;  $\beta$ -galactosidase stained culture dishes representing maximal dose of FSP27 (*left*) and empty vector controls (*right*) are shown beneath the graph.

We also sought to compare the level of FSP27 expression that we expressed in transient transfection assays and that we had demonstrated to promote apoptosis, with the level of FSP27 normally found in white adipocytes. To do so we used

RT-PCR to determine the FSP27 transcript level for 293T cells at various time points posttransfection with an FSP27 expression construct and compared it with that present in WAT and in 3T3-L1 cells that had been subjected to the adipocyte differentiation protocol (Fig. 8E). Transfection studies were conducted under the same conditions utilized for Fig. 8, A–C. To be able to compare the FSP27 transcript expression level in the transfected cells within the 293T cell population with that in adipocytes, we conducted parallel transfection of 293T cells with a Lac-Z expression construct.  $\beta$ -galactosidase staining of these parallel cultures indicated a 70% transfection efficiency. In regard to the percentage of adipocytes in either the WAT sample or the differentiated 3T3-L1 cell sample, it has been reported that the percentage of adipocytes in whole WAT is

between one-third and two-thirds (1); thus we estimated that ~50% of the cells in the WAT sample were fat cells. Adipocytes make up ~85% of the differentiated 3T3-L1 cultures. The plotted data for the FSP27 transcript level, after correction for the percent transfection of the 293T cell population and the percentage of adipocytes in either the WAT or differentiated 3T3-L1 cell populations, is shown in Fig. 8E. At no time from 4 h through 24 h posttransfection does the level of ectopically expressed the FSP27 transcript appreciably exceed that detected in adipocytes from WAT or 3T3-L1 adipocytes. Our data thus support the conclusion that compared with the FSP27 transcript level that is normally expressed by adipocytes, ectopic expression of FSP27 in 293T cells, at all posttransfection time points tested, is similar to that found in WAT, while FSP27 clearly leads to cell death in the former case. One caveat to this is the possibility that those transfected cells that express extremely high levels of the FSP27 transcript have rapidly died off and are thus no longer within the population of cells we have assessed.

*FSP27 promotes preadipocyte cell death.* We reasoned that since white adipocytes express a high level of FSP27, that perhaps if a role of this molecule in these cells were mediating adipocyte apoptosis, we would see an increase in basal apoptotic rate in adipocytes vs. preadipocytes. Figure 9A indicates that neither 3T3-L1 preadipocytes nor 3T3-L1 adipocytes evidence detectable apoptosis under normal culture conditions, as demonstrated by the lack of DNA laddering. Thus the induction of expression of FSP27 that occurs during adipogenesis does not, in that context, result in increased cellular apoptosis. This is generally in line with the observations that adipocytes are relatively resistant to apoptosis, at least when studied under the specific conditions of growth factor withdrawal (52). To confirm that mature 3T3-L1 adipocytes indeed express FSP27 protein while preadipocytes do not, we conducted Western blot analysis. As shown in Fig. 9B, a dramatic induction of FSP27 protein expression occurs in mature adipocytes, with a major protein species in good agreement with the predicted molecular mass of 27.3 kDa for FSP27. We also note two minor, faster migrating species of the protein. It is possible that the smallest of these may be a product of alternate splicing. Human FSP27 has been reported to be present as two transcripts; the smaller of which generates a protein consistent with that we note (28). However, our search for identification of alternate FSP27 transcripts from murine adipocytes did not indicate the presence of shorter form(s) of the transcript (data not shown). Interestingly, during our studies on the FSP27 protein, we have found that the size of the FSP27 protein species detected varied

when the protein possessed an NH<sub>2</sub>-terminal vs. a COOH-terminal epitope tag. To further address this observation, we created an expression construct for FSP27 that contained two distinct epitope tags, an NH<sub>2</sub>-terminal HA tag and a COOH-terminal FLAG tag. Figure 9C shows that use of the anti-HA antibody to detect the NH<sub>2</sub>-terminal HA tag results in a single

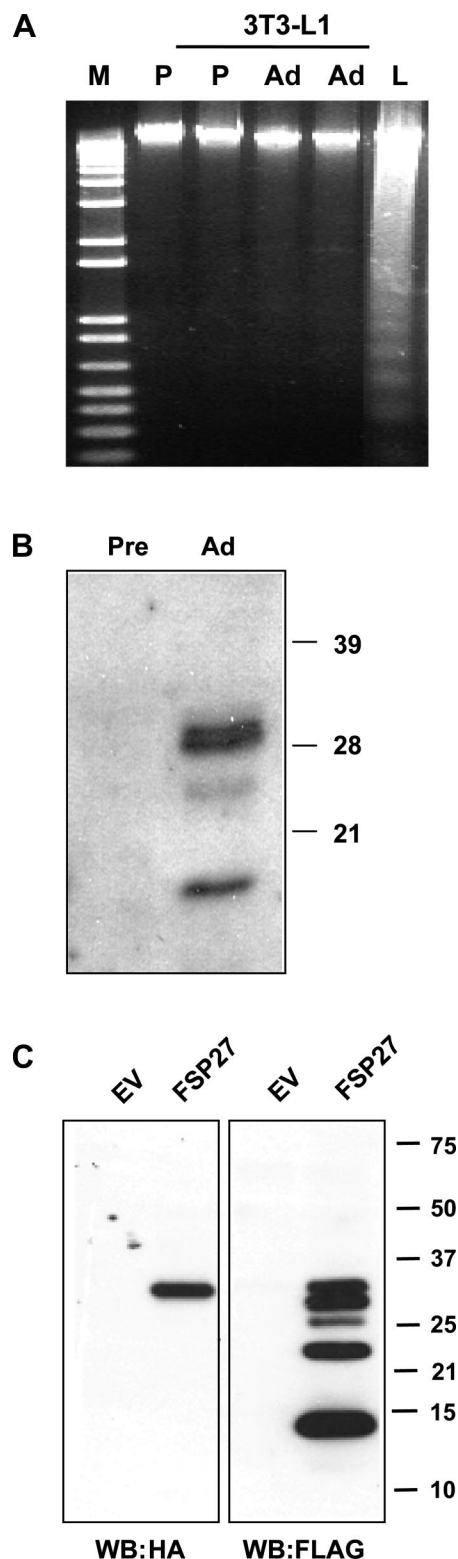


Fig. 9. Assessment of FSP27 apoptotic activity and protein expression in the adipocyte (P) lineage. **A:** DNA fragmentation assay in 3T3L1 preadipocytes (P) and adipocytes. Genomic DNA prepared from duplicate cultures of preadipocytes (P) or adipocyte (Ad) and assessed by electrophoresis through 1.2% agarose gels. A control apoptotic ladder (L) is shown at right, and DNA marker (M) is shown at far left; data shown here were obtained from the same original image of an agarose gel; however, some data lanes were either removed or rearranged for economy and/or clarity of presentation. **B:** Western blot analysis of 30 µg cell lysate of 3T3-L1 preadipocytes (Pre) or Ad with FSP27 antibody. **C:** Western blot analysis of cell lysates of 30 µg of cell lysates from transfection of COS cells with a double epitope tag FSP27 expression construct, bearing an NH<sub>2</sub>-terminal HA tag and a COOH-terminal FLAG tag or with empty vector (EV). Both panels shown are from a single transfer where the membrane was cut vertically such that one portion was subject to Western blot with anti-HA antibody and the other with anti-FLAG antibody.

protein species consistent in mass with that predicted for the FSP27 open reading frame. In contrast, use of the anti-FLAG antibody to detect the COOH-terminal FLAG tag results in full-length FSP27 protein as well as several distinct smaller protein species. Future work will more fully address the nature and function of the full-length and multiple shorter forms of the FSP27 protein. We do not at this time know what regions shorter forms of FSP27 may represent. However, since the smallest of these are approximately half the mass of full-length FSP27, we hypothesize that this might correspond to the Cide C domain; in studies of CIDEB, it is the Cide C domain that has been illustrated to be necessary and sufficient for apoptosis (7). These observations imply that the various FSP27 protein species might represent different functional forms.

We next investigated the ability of preadipocytes to undergo FSP27-mediated cell death using ectopic expression of FSP27 in 3T3-L1 preadipocytes wherein empty vector or FSP27 transfected cells are visualized as blue via cotransfection of a LacZ expression construct, as previously used for 293T cells (Fig. 8). Since compared with 293T cells, 3T3-L1 preadipocytes exhibit markedly reduced transfection efficiency, for these studies the mass of LacZ expression construct utilized was increased. Here the ratio of FSP27 to LacZ expression construct was only 3:1, rather than the small amount of tracer LacZ plasmid used with 293T cells in Fig. 8. Figure 10A shows that relative to empty vector transfectants, 3T3-L1 preadipocytes transfected with an FSP27 expression construct evidenced a statistically significant  $\sim 20\%$  decrease ( $P < 0.05$ ) in cell number. When these same transfection conditions were applied to 293T cells, they showed a similar  $\sim 20\%$  decrease ( $P < 0.05$ ) in cell number, indicating that FSP27 is equally effective at promoting cell death in 3T3-L1 preadipocytes as for 293T cells. Figure 10B illustrates the cell death effect of FSP27 in 3T3-L1 preadipocytes by  $\beta$ -galactosidase staining assay that utilized a 6:1 ratio of FSP27 to LacZ expression construct. A representative microscopic field of a culture dish is shown; transfection efficiency was too low to allow visualization of  $\beta$ -galactosidase staining by macroscopic view of culture dishes. We have also observed the cell death effect in CHO cells, where the majority of  $\beta$ -galactosidase-positive cells appear as small apoptotic bodies in the FSP27-transfected cultures vs. the normal morphological appearance of cells transfected with empty vector. With the use of an EGFP-tagged FSP27 protein, Fig. 10C illustrates that cells harboring this fusion protein are clearly undergoing apoptosis, illustrated by membrane blebbing and loss of cellular integrity (*top*) and by nuclear condensation as detected by staining with Hoechst dye (*bottom*). The cellular morphology and nuclear staining intensity of empty EGFP vector control transfectants were indistinguishable from nontransfected cells (data not shown). When we examined EGFP-FSP27-transfected COS cells or 3T3-L1 preadipocytes at time points later than  $\sim 30$  h posttransfection, we had difficulty finding any EGFP-positive cells in the transfected population; those that were present had a small circular morphology indicative of late-stage apoptosis or were round, floating, and presumably dead cells (data not shown).

**Localization studies of FSP27 protein.** Our data clearly indicate that misexpression of FSP27 in cells other than adipocytes can trigger apoptosis accompanied by several key apoptotic hallmarks. The precise mechanism of this apoptotic action is not yet known; however, the reported localization of

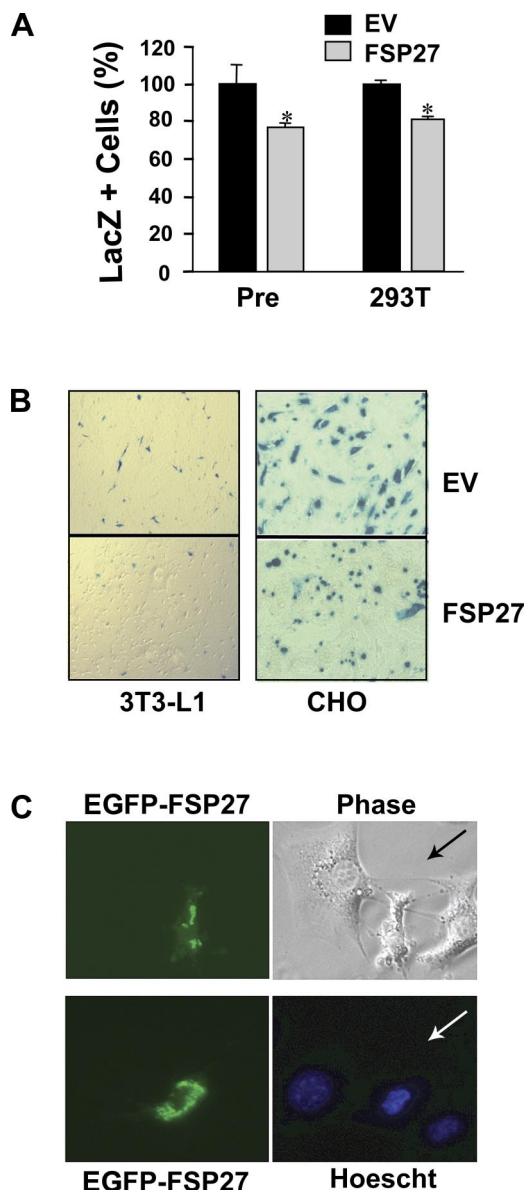


Fig. 10. Cell death effects of FSP27. **A**: cell death assay of 3T3-L1 preadipocytes (pre) and 293T cells (293T) of cells transfected with EV or a murine FSP27 expression construct (1.5  $\mu$ g) in combination with a LacZ expression construct (0.5  $\mu$ g). Cells were enumerated as described in MATERIALS AND METHODS, and cell viability in EV transfectants was set to 100% ( $*P < 0.05$ ). **B**: images of microscopic field of  $\beta$ -galactosidase stained cells of preadipocytes (*left*) or CHO cells (*right*) transfected with 0.5  $\mu$ g of a lacZ expression construct in combination with 3.5  $\mu$ g of EV or an FSP27 expression construct. Cells were stained at 48 posttransfection. **C**: 3T3-L1 preadipocytes were transfected with an enhanced green fluorescent protein (EGFP)-FSP27 fusion construct and observed by fluorescence (dark panels) for EGFP signal and Hoechst-stained nuclei and phase microscopy as indicated. Black arrow indicates typical morphology of transfected cells at 48 h posttransfection; white arrow indicates bright Hoechst staining indicative of condensed chromatin.

FSP27, as well as CIDEA and CIDEB, to mitochondria would appear to indicate that FSP27 may initiate apoptosis via mitochondrial signals. While this article was in revision, it was reported by Puri et al. (39) that FSP27 is a lipid droplet associated molecule; these authors also indicated lack of mitochondrial localization for FSP27 in contrast to an earlier report (29). Both of these studies utilized the same type of

EGFP fusion proteins and MitoTracker probes for their analysis, with the latter assessing human FSP27 and the former murine FSP27. Since the localization of FSP27 is key to its functional consequences in both adipocyte physiology and apoptosis, we had also carried out studies on the localization of human EGFP-FSP27 in COS cells and 3T3-L1 preadipocytes by confocal microscopy (Supplemental Fig. 1; the online version of this article contains supplemental data). An extremely low transfection efficiency of 3T3-L1 adipocytes and the ineffectiveness of the FSP27 antibody for immunocytochemistry precluded a definitive study on FSP27 protein localization in adipocytes in our hands. However, our observations in COS and 3T3-L1 preadipocytes indicated only an extremely limited degree of colocalization of FSP27 with MitoTracker Red; this is particularly apparent in the individual 0.5- $\mu$ m Z-sections.

All MitoTracker probes are to some extent dependent on intact mitochondrial membrane potential for fluorescence intensity. Given that the effects of FSP27 on mitochondrial membrane potential are not known, we therefore also assessed localization by transfection of an organelle-specific fluorophore that is not known to be affected by mitochondrial membrane potential. The pDSRed-2 protein is directed to specifically localize to mitochondria via the addition of a mitochondrial targeting signal; this method also failed to indicate mitochondrial localization (Supplemental Fig. 2). However, we have routinely observed that expression of FSP27 in COS cells leads to disruption of the mitochondria from a fine spaghetti-like filaments that are normally present in these cells to a disordered appearance (Supplementary Fig. 3). This suggests the possibility of a role for mitochondria in the proapoptotic action of FSP27, as has been indicated in studies of CIDEA (8).

## DISCUSSION

The regulation we describe for the FSP27 transcript is wholly consistent with the recent report that in adipocytes FSP27 acts to support energy storage. FSP27 protein has been reported to be localized surrounding adipocyte lipid droplets in a pattern reminiscent of that for the well-characterized lipid droplet protein perilipin (39). Our observations that the FSP27 transcript is upregulated by insulin and diminished by TNF- $\alpha$  suggest that not only the function of the protein per se but that a coordinated transcript regulation is also involved in the antilipolytic and proenergy storage effects of FSP27. On the other hand, the regulation we find for the FSP27 transcript in adipocytes is at apparent odds with the role of TNF- $\alpha$  and insulin in cellular apoptosis and cell survival. TNF- $\alpha$  is a well-described proapoptotic cytokine in a number of cell types including adipocytes (29, 35, 37, 38, 40, 50). With the caveat that many of the control points in apoptotic signaling are at the level of protein processing and interaction, one might nonetheless anticipate that if the central role of FSP27 were in the stimulation/mediation of apoptosis, then pro- and antiapoptotic agents would modulate the FSP27 transcript level accordingly. In this regard, TNF- $\alpha$  would be predicted to increase, rather than decrease, FSP27 level. Importantly, we have discovered that the FSP27 transcript is a target for rapid and robust upregulation by insulin. Surprisingly, given the central role of insulin in adipocyte function, there are relatively few studies that have systematically addressed the effects of insulin on

global adipocyte gene expression (34, 49). To our knowledge, we are the first to present data describing insulin upregulation of the FSP27 transcript. Insulin is generally a prosurvival factor and has been demonstrated to inhibit adipocyte apoptosis (37, 40). As such, insulin might be predicted to decrease expression of proapoptotic genes, but we observed a dramatic upregulation of the FSP27 transcript by insulin. As insulin is well established to promote lipid storage in fat cells, upregulation FSP27 by insulin may be a type of protective mechanism whereby the cell is assured it has adequate levels of this particular lipid droplet protein to sufficiently handle the increased lipid storage that occurs as a consequence of the prolipogenic effects of insulin on adipocytes.

Puri et al. (39) recently showed that knockdown of FSP27 in adipocytes was reported to lead to fragmentation of large lipid droplets into abundant small droplets and that ectopic expression of FSP27 in 3T3-L1 preadipocytes, as well as in COS and CHO cells, leads to the accumulation of lipid droplets. While we have not assessed lipid droplet accumulation as the result of ectopic FSP27 expression, we have demonstrated that ectopic FSP27 promotes apoptosis. It remains to be investigated whether the ectopic accumulation of lipid that is mediated by FSP27 is a step in the apoptotic mechanism for FSP27; however, the lipotoxic and apoptotic effect of lipids have been clearly documented in a number of physiological settings (56, 57). This also raises the interesting point of what might occur when FSP27 is upregulated in cells that lack the appropriate lipid droplet milieu found in the adipocyte; our data would support the notion that such cells might be prone to apoptotic cell death. That we do not observe an increase in basal DNA fragmentation upon adipocyte differentiation, despite the dramatic upregulation of FSP27 that occurs in adipogenesis, leads to the hypothesis that perhaps various protein-protein interactions that occur in the adipocyte lineage might function to keep the proapoptotic activity of FSP27 in check. In light of the recent study (39) indicating that FSP27 is a lipid droplet associated protein, one might postulate that some of these interactions occur at the lipid droplet.

Overall, our studies on the localization of FSP27 in transfected COS cells are in line with those reported by Puri et al. (39), in that we do not find convincing evidence of mitochondrial localization. In the discussion section of that report, the authors indicated that in light of their data indicating that FSP27 is a lipid droplet protein rather than a mitochondrial protein, they thought it would be interesting to further explore the current working hypothesis for CIDEA action, namely the ability of CIDEA to apparently inhibit the action of the mitochondrial UCPI (thought to be the basis for the lean phenotype of CIDEA-null mice); might CIDEA also be a lipid droplet associated protein? We would agree that this needs further exploration, particularly since we have observed by yeast two-hybrid and biochemical methods that FSP27 and CIDEA interact (data not shown), which would support the notion that these proteins might share a similar intracellular localization.

Until relatively recently it was thought that adipose number in human was constant from young adulthood onward. Over the last several decades with the remarkable progress in the study of adipogenesis, it is now accepted that adipocyte differentiation is an ongoing process throughout the life span (17, 51). More recently, it has become clear that in addition to adipocyte hypertrophy and hyperplasia, fat cell mass can also

be effected by adipocyte or preadipocyte apoptosis (52). The balance between differentiation, growth, and cell death of the adipocyte lineage is therefore key to determining whether the number of fat cells an individual has is sufficient for optimal health or a burden that leads to diabetes, heart disease, and associated morbidities. It is intriguing to speculate that under certain conditions wherein adipocyte apoptosis is required, cellular mechanisms may exist for the activation of cell death-promoting activities of FSP27 in adipocytes. Likewise, if pathways for the activation of the cell death-promoting aspects of FSP27 function in mature adipocytes were discovered, this might provide a therapeutic intervention point at which to target reduction of fat cell mass and combat obesity.

#### ACKNOWLEDGMENTS

We thank D. Sowa for excellent technical assistance. We also thank D. Giovannucci (University of Toledo Health Science Campus) and members of his laboratory for contributing expertise in confocal microscopy.

#### GRANTS

This work was supported by the University of Toledo Health Science Campus.

#### REFERENCES

- Ailhaud G, Hauner H. Development of white adipose tissue. In: *Handbook of Obesity, Etiology and Pathophysiology*, edited by Bray GA and Bouchard C. New York, NY: Marcel Dekker, 2004.
- Birkenmeier EH, Gwynn B, Howard S, Jerry J, Gordon JI, Landschulz WH, McKnight SL. Tissue-specific expression, developmental regulation, and genetic mapping of the gene encoding CCAAT/enhancer binding protein. *Genes Dev* 3: 1146–1156, 1989.
- Boone C, Mouro J, Gregoire F, Remacle C. The adipose conversion process: regulation by extracellular and intracellular factors. *Reprod Nutr Dev* 40: 325–358, 2000.
- Bradley RL, Cleveland KA, Cheatham B. The adipocyte as a secretory organ: mechanisms of vesicle transport and secretory pathways. *Recent Prog Horm Res* 56: 329–358, 2001.
- Brasaemle DL, Dolios G, Shapiro L, Wang R. Proteomic analysis of proteins associated with lipid droplets of basal and lipolytically stimulated 3T3-L1 adipocytes. *J Biol Chem* 279: 46835–46842, 2004.
- Chapman AB, Knight DM, Dieckmann BS, Ringold GM. Analysis of gene expression during differentiation of adipogenic cells in culture and hormonal control of the developmental program. *J Biol Chem* 259: 15548–15555, 1984.
- Chapman AB, Knight DM, Ringold GM. Glucocorticoid regulation of adipocyte differentiation: hormonal triggering of the developmental program and induction of a differentiation-dependent gene. *J Cell Biol* 101: 1227–1235, 1985.
- Chen Z, Guo K, Toh SY, Zhou Z, Li P. Mitochondria localization and dimerization are required for CIDE-B to induce apoptosis. *J Biol Chem* 275: 22619–22622, 2000.
- Coppack SW. Pro-inflammatory cytokines and adipose tissue. *Proc Nutr Soc* 60: 349–356, 2001.
- Dahlman I, Kaaman M, Jiao H, Kere J, Laakso M, Arner P. The CIDEA gene V115F polymorphism is associated with obesity in Swedish subjects. *Diabetes* 54: 3032–3034, 2005.
- Danesch U, Hoek W, Ringold GM. Cloning and transcriptional regulation of a novel adipocyte-specific gene, FSP27. CAAT-enhancer-binding protein (C/EBP) and C/EBP-like proteins interact with sequences required for differentiation-dependent expression. *J Biol Chem* 267: 7185–7193, 1992.
- Darlington GJ, Ross SE, MacDougald OA. The role of C/EBP genes in adipocyte differentiation. *J Biol Chem* 273: 30057–30060, 1998.
- Ding HF, Lin YL, McGill G, Joo P, Zhu H, Blenis J, Yuan J, Fisher DE. Essential role for caspase-8 in transcription-independent apoptosis triggered by p53. *J Biol Chem* 275: 38905–38911, 2000.
- Forman BM, Tontonoz P, Chen J, Brun RP, Spiegelman BM, Evans RM. 15-Deoxy-delta 12, 14-prostaglandin J2 is a ligand for the adipocyte determination factor PPAR gamma. *Cell* 83: 803–812, 1995.
- Green H, Kehinde O. An established preadipose cell line and its differentiation in culture. II Factors affecting the adipose conversion. *Cell* 5: 19–27, 1975.
- Gregoire FM. Adipocyte differentiation: from fibroblast to endocrine cell. *Exp Biol Med (Maywood)* 226: 997–1002, 2001.
- Gregoire FM, Smas CM, Sul HS. Understanding adipocyte differentiation. *Physiol Rev* 78: 783–809, 1998.
- Gummeson A, Jernas M, Svensson PA, Larsson I, Glad CA, Schele E, Gripeteg L, Sjöholm K, Lystig TC, Sjöström L, Carlsson B, Fagerberg B, Carlsson LM. Relations of adipose tissue cell death-inducing DFFA-like effector A gene expression to basal metabolic rate, energy restriction and obesity: population-based and dietary intervention studies. *J Clin Endocrinol Metab* 92: 4759–4765, 2007.
- Havel PJ. Control of energy homeostasis and insulin action by adipocyte hormones: leptin, acylation stimulating protein, and adiponectin. *Curr Opin Lipidol* 13: 51–59, 2002.
- Inohara N, Koseki T, Chen S, Wu X, Nunez G. CIDE, a novel family of cell death activators with homology to the 45 kDa subunit of the DNA fragmentation factor. *EMBO J* 17: 2526–2533, 1998.
- Inohara N, Nunez G. Genes with homology to DFF/CIDEs found in *Drosophila melanogaster*. *Cell Death Differ* 6: 823–824, 1999.
- Kelder B, Boyce K, Kriete A, Clark R, Berryman DE, Nagatomi S, List EO, Braugher M, Kopchick JJ. CIDE-A is expressed in liver of old mice and in type 2 diabetic mouse liver exhibiting steatosis. *Comp Hepatol* 6: 4, 2007.
- Kim S, Moustaid-Moussa N. Secretory, endocrine and autocrine/paracrine function of the adipocyte. *J Nutr* 130: 3110S–3115S, 2000.
- Klein J, Fasshauer M, Klein HH, Benito M, Kahn CR. Novel adipocyte lines from brown fat: a model system for the study of differentiation, energy metabolism, and insulin action. *Bioessays* 24: 382–388, 2002.
- Knight DM, Chapman AB, Navre M, Drinkwater L, Bruno JJ, Ringold GM. Requirements for triggering of adipocyte differentiation by glucocorticoids and indomethacin. *Mol Endocrinol* 1: 36–43, 1987.
- Laborda J. 36B4 cDNA used as an estradiol-independent mRNA control is the cDNA for human acidic ribosomal phosphoprotein PO. *Nucleic Acids Res* 19: 3998, 1991.
- Li JZ, Ye J, Xue B, Qi J, Zhang J, Zhou Z, Li Q, Wen Z, Li P. Cideb regulates diet-induced obesity, liver steatosis, and insulin sensitivity by controlling lipogenesis and fatty acid oxidation. *Diabetes* 56: 2523–2532, 2007.
- Li P. Cidea, brown fat and obesity. *Mech Ageing Dev* 125: 337–338, 2004.
- Liang L, Zhao M, Xu Z, Yokoyama KK, Li T. Molecular cloning and characterization of CIDE-3, a novel member of the cell-death-inducing DNA-fragmentation-factor (DFF45)-like effector family. *Biochem J* 370: 195–203, 2003.
- Lin SC, Li P. CIDE-A, a novel link between brown adipose tissue and obesity. *Trends Mol Med* 10: 434–439, 2004.
- Lugovskoy AA, Zhou P, Chou JJ, McCarty JS, Li P, Wagner G. Solution structure of the CIDE-N domain of CIDE-B and a model for CIDE-N/CIDE-N interactions in the DNA fragmentation pathway of apoptosis. *Cell* 99: 747–755, 1999.
- MacDougald OA, Mandrup S. Adipogenesis: forces that tip the scales. *Trends Endocrinol Metab* 13: 5–11, 2002.
- Mueller E, Drori S, Aiyer A, Yie J, Sarraf P, Chen H, Hauser S, Rosen ED, Ge K, Roeder RG, Spiegelman BM. Genetic analysis of adipogenesis through peroxisome proliferator-activated receptor gamma isoforms. *J Biol Chem* 277: 41925–41930.
- Mulligan C, Rochford J, Denyer G, Stephens R, Yeo G, Freeman T, Siddle K, O'Rahilly S. Microarray analysis of insulin and insulin-like growth factor-1 (IGF-1) receptor signaling reveals the selective up-regulation of the mitogen heparin-binding EGF-like growth factor by IGF-1. *J Biol Chem* 277: 42480–42487, 2002.
- Niesler CU, Siddle K, Prins JB. Human preadipocytes display a depot-specific susceptibility to apoptosis. *Diabetes* 47: 1365–1368, 1998.
- Nordstrom EA, Ryden M, Backlund EC, Dahlman I, Kaaman M, Blomqvist L, Cannon B, Nedergaard J, Arner P. A human-specific role of cell death-inducing DFFA (DNA fragmentation factor-alpha)-like effector A (CIDEA) in adipocyte lipolysis and obesity. *Diabetes* 54: 1726–1734, 2005.
- Prins JB, Niesler CU, Winterford CM, Bright NA, Siddle K, O'Rahilly S, Walker NI, Cameron DP. Tumor necrosis factor-alpha induces apoptosis of human adipose cells. *Diabetes* 46: 1939–1944, 1997.
- Prins JB, O'Rahilly S. Regulation of adipose cell number in man. *Clin Sci (Lond)* 92: 3–11, 1997.

39. Puri V, Konda S, Ranjit S, Aouadi M, Chawla A, Chouinard M, Chakladar A, Czech MP. Fat specific protein 27: A novel lipid droplet protein that enhances triglyceride storage. *J Biol Chem* 282: 34213–34218, 2007.
40. Qian H, Hausman DB, Compton MM, Martin RJ, Della-Fera MA, Hartzell DL, Baile CA. TNF $\alpha$  induces and insulin inhibits caspase 3-dependent adipocyte apoptosis. *Biochem Biophys Res Commun* 284: 1176–1183, 2001.
41. Rajala MW, Scherer PE. Minireview: The adipocyte—at the crossroads of energy homeostasis, inflammation, and atherosclerosis. *Endocrinology* 144: 3765–3773, 2003.
42. Rosen ED, Hsu CH, Wang X, Sakai S, Freeman MW, Gonzalez FJ, Spiegelman BM. C/EBP $\alpha$  induces adipogenesis through PPAR $\gamma$ : a unified pathway. *Genes Dev* 16: 22–26, 2002.
43. Rosen ED, Sarraf P, Troy AE, Bradwin G, Moore K, Milstone DS, Spiegelman BM, Mortensen RM. PPAR $\gamma$  is required for the differentiation of adipose tissue in vivo and in vitro. *Mol Cell* 4: 611–617, 1999.
44. Rosen ED, Spiegelman BM. Molecular regulation of adipogenesis. *Annu Rev Cell Dev Biol* 16: 145–171, 2000.
45. Rosen ED, Spiegelman BM. PPAR $\gamma$ : a nuclear regulator of metabolism, differentiation, and cell growth. *J Biol Chem* 276: 37731–37734.
46. Rosen ED, Walkey CJ, Puigserver P, Spiegelman BM. Transcriptional regulation of adipogenesis. *Genes Dev* 14: 1293–1307, 2000.
47. Ruan H, Hacohen N, Golub TR, Van Parijs L, Lodish HF. Tumor necrosis factor- $\alpha$  suppresses adipocyte-specific genes and activates expression of preadipocyte genes in 3T3-L1 adipocytes: nuclear factor- $\kappa$ B activation by TNF- $\alpha$  is obligatory. *Diabetes* 51: 1319–1336, 2002.
48. Ruan H, Miles PD, Ladd CM, Ross K, Golub TR, Olefsky JM, Lodish HF. Profiling gene transcription in vivo reveals adipose tissue as an immediate target of tumor necrosis factor- $\alpha$ : implications for insulin resistance. *Diabetes* 51: 3176–3188, 2002.
49. Sartipy P, Loskutoff DJ. Expression profiling identifies genes that continue to respond to insulin in adipocytes made insulin-resistant by treatment with tumor necrosis factor- $\alpha$ . *J Biol Chem* 278: 52298–52306.
50. Sethi JK, Hotamisligil GS. The role of TNF $\alpha$  in adipocyte metabolism. *Semin Cell Dev Biol* 10: 19–29, 1999.
51. Smas CM, Sul HS. Control of adipocyte differentiation. *Biochem J* 309: 697–710, 1995.
52. Sorisky A, Magun R, Gagnon AM. Adipose cell apoptosis: death in the energy depot. *Int J Obes Relat Metab Disord* 24, Suppl 4: S3–S7, 2000.
53. Souza SC, Palmer HJ, Kang YH, Yamamoto MT, Muliro KV, Paulson KE, Greenberg AS. TNF- $\alpha$  induction of lipolysis is mediated through activation of the extracellular signal related kinase pathway in 3T3-L1 adipocytes. *J Cell Biochem* 89: 1077–1086, 2003.
54. Torti FM, Torti SV, Larrick JW, Ringold GM. Modulation of adipocyte differentiation by tumor necrosis factor and transforming growth factor beta. *J Cell Biol* 108: 1105–1113, 1989.
55. Umek RM, Friedman AD, McKnight SL. CCAAT-enhancer binding protein: a component of a differentiation switch. *Science* 251: 288–292, 1991.
56. Unger RH. Minireview: weapons of lean body mass destruction: the role of ectopic lipids in the metabolic syndrome. *Endocrinology* 144: 5159–5165.
57. Unger RH, Orci L. Lipotoxic diseases of nonadipose tissues in obesity. *Int J Obes Relat Metab Disord* 24, Suppl 4: S28–S32, 2000.
58. Viswakarma N, Yu S, Naik S, Kashireddy P, Matsumoto K, Sarkar J, Surapureddi S, Jia Y, Rao MS, Reddy JK. Transcriptional regulation of Cidea, mitochondrial cell death-inducing DNA fragmentation factor alpha-like effector A, in mouse liver by peroxisome proliferator-activated receptor alpha and gamma. *J Biol Chem* 282: 18613–18624, 2007.
59. Williams PM, Chang DJ, Danesch U, Ringold GM, Heller RA. CCAAT/enhancer binding protein expression is rapidly extinguished in TA1 adipocyte cells treated with tumor necrosis factor. *Mol Endocrinol* 6: 1135–1141, 1992.
60. Wu Z, Rosen ED, Brun R, Hauser S, Adelmant G, Troy AE, McKeon C, Darlington GJ, Spiegelman BM. Cross-regulation of C/EBP $\alpha$  and PPAR $\gamma$  controls the transcriptional pathway of adipogenesis and insulin sensitivity. *Mol Cell* 3: 151–158, 1999.
61. Wu Z, Xie Y, Bucher NL, Farmer SR. Conditional ectopic expression of C/EBP $\beta$  in NIH-3T3 cells induces PPAR $\gamma$  and stimulates adipogenesis. *Genes Dev* 9: 2350–2363, 1995.
62. Xing H, Northrop JP, Grove JR, Kilpatrick KE, Su JL, Ringold GM. TNF $\alpha$ -mediated inhibition and reversal of adipocyte differentiation is accompanied by suppressed expression of PPAR $\gamma$  without effects on Pref-1 expression. *Endocrinology* 138: 2776–2783, 1997.
63. Yu S, Matsusue K, Kashireddy P, Cao WQ, Yeldandi V, Yeldandi AV, Rao MS, Gonzalez FJ, Reddy JK. Adipocyte-specific gene expression and adipogenic steatosis in the mouse liver due to peroxisome proliferator-activated receptor gamma1 (PPAR $\gamma$ 1) overexpression. *J Biol Chem* 278: 498–505, 2003.
64. Zhou Z, Yon Toh S, Chen Z, Guo K, Ng CP, Ponniah S, Lin SC, Hong W, Li P. Cidea-deficient mice have lean phenotype and are resistant to obesity. *Nat Genet* 35: 49–56, 2003.